Diesel fuel particulate emissions from a constant-volume combustion chamber

Sofia Törmä

Master´s thesis for the degree of Master of Science in Technology

Laboratory of Inorganic Chemistry, Faculty of Science and Engineering

Åbo Akademi University

ÅBO AKADEMI UNIVERSITY – FACULTY OF SCIENCE AND ENGINEERING

Abstract for Master's thesis

Subject: Process chemistry		
Author: Sofia Törmä		
Title: Diesel fuel particulate emissions from a constant-volume combustion chamber		
Supervisor: Tor Laurén	**Supervisor**: Sofia Nystén	**Supervisor**: Leena Hupa

Abstract:

In January 2017 the European Commission published a new Best Available Technique (BAT) Reference Document for Large Combustion Plants (LCP). The document is aimed for combustion installations over 50 MW rated thermal input. The emission limit of particulate matter tightened to 10 mg/Nm^3 (at 15 vol-% O_2). Currently, this limit is only possible to reach (without exhaust gas cleaning) with high-quality light fuel oil (LFO) in Wärtsilä engines.

The aim of this work was to measure how fuel properties influence the particle mass (PM) concentration in a constant-volume chamber, a Combustion Research Unit (CRU) made by Fueltech. The aim was realized in pilot tests on the CRU. In addition, the pilot-scale tests were compared to particulate emissions from a medium-speed diesel engine. Light fuel oil (LFO) was the main fuel considered throughout the work. The area of study was motivated by the low number of previous studies that quantitatively measure PM from a constant-volume chamber.

The fuel properties of interest were density, sulphur and oxygen content. PM was expected to increase with density and sulphur content, while the opposite behaviour was anticipated for increasing oxygen content. Unfortunately, the pilot tests were unable to produce repeatable, coherent results. No difference in particulate release could be distinguished between light and heavy fuel oils. The disparity was caused by the deficient measurement setups, and particles were either lost or modified between the combustion chamber and the detector, an electrical low-pressure impactor (ELPI) by Dekati Ltd.. Identified factors that influenced the results were thermophoresis, inertial impaction, settling, uncontrolled dilution and insufficient sample amount. No conclusions could be drawn concerning the influence of fuel properties on particulate release.

A Wärtsilä W6L32 engine was operated on LFO and 100 % load. Both in-stack ISO 9096 and double-diluted ELPI were used to measure total dust. In the test conditions ELPI measurements gave around 50 % lower particulate mass results than the ISO 9096 method. The discrepancies were concluded to originate from the fundamental difference in how particles were measured and from the dilution conditions.

The comparison between the engine and the CRU deduced that the engine particle emissions by ELPI and ISO 9096 were 67 % respectively 35 % less than CRU particle release. The discrepancy was concluded to originate from the in-cylinder conditions

(higher temperature and pressure) in the engine and due to the poorer fuel-air mixing in the static combustion chamber.

The opportunity to perform fuel tests in small scale is valuable for understanding fuel combustion behaviour and particle emissions. For future particle measurements on the CRU it was advised to remove all valves and sharp duct bends. Further, heated duct walls, controlled and monitored dilution, and collection of entire CRU exhaust were recommended.

Key words: particulate mass, ELPI, medium-speed engine, light-fuel oil, constant-volume combustion chamber

Date: 19.02.2019	Number of pages: 66

Abstraktet godkänt som mognadsprov:

Svensk Sammanfattning

Stoftutsläpp från dieselmotorer har den senaste tiden varit utsatt för intensiv debatt. Det vanligaste och synligaste användningsområdet av dieselmotorer är bilar. Övriga användningsområden av dieselmotorer är i fartyg och i elproduktion. I december 2017 publicerade EU kommissionen en uppdatering på BAT-dokumentet (Best Available Technique) för förbränningsanläggningar med en sammanlagd tillförd termisk effekt på över 50 MW. Uppdateringen innehöll bland annat en ny utsläppsgräns för stoft som nya anläggningar är tvungna att följa. Den nya stoftgränsen är 10 mg/Nm^3 (i 15 vol-% syre). För tillfället når Wärtsiläs motorer detta krav utan avgasrening endast med lätt brännolja av hög kvalitet. För att säkerställa att Wärtsilä når utsläppsgränserna även i framtiden, krävs ytterligare information om hur bränslet påverkar uppkomsten av stoft.

Ändamålet med arbetet var att studera vilka bränsleegenskaper i lätt brännolja som påverkar massakoncentrationen stoft i en statisk förbränningskammare. Förbränningskammaren i fråga var tillverkad av Fueltech och benämns i detta arbete som CRU (Combustion Research Unit). Utöver testerna i pilotskala utfördes stoftmätningar på en W6L32 motor. Parallella mätningar med en standardiserad metod (ISO 9096) och en ELPI (electrical low-pressure impactor) av märket Dekati Ltd. användes för att mäta massakoncentrationen av stoft i motoravgaserna. Det andra ändamålet var att uppskatta skillnaden i stoftutsläpp mellan CRU:n och en motor. Väldigt få tidigare undersökningar har kvantitativt mätt stoftmassa från en motsvarande förbränningskammare och lätt brännolja.

Den vanligaste metoden för att bestämma stoftutsläpp är gravimetrisk, d.v.s uppvägning av samlad stoftmassa. Även lagstadgade och standardiserade metoder, såsom ISO 9096 och EN13284-1:2017, baserar sig på massa. Nackdelen med filterbaserade metoder är att de huvudsakligen fångar upp stora stoftpartiklar. Samtidigt är små partiklar studerat farligare för hälsan. Eftersom små partiklar knappt har någon massa, är filtermetoden otymplig. Ett alternativ för mätning av små partiklar är definiering av partikelantal. Europaparlamentets och rådets förordning (EU) 2016/1628 om krav för utsläppsgränser vad gäller gas- och partikelformiga föroreningar samt typgodkännande av

förbränningsmotorer för mobila maskiner som inte är avsedda att användas för transporter på väg[1], beskriver att partikelantalet för fartygsmotorer i inlandssjöfart begränsas till 1×10^{12}/kWh. Partikelantalet gäller för fasta partiklar med en diameter större än 23 nm. En motsvarande begränsning saknas för landbaserade kraftverksmotorer. Orsaken är att partikelantalmätning har hög osäkerhet, låg repeterbarhet och metoden är bättre lämpad för små motorer.

På basis av litteraturstudien valdes tre bränsleegenskaper för närmare granskning i den experimentella delen. Litteraturstudien illustrerade det knepiga i att försöka isolera en enda bränsleegenskap som bidrar mest till stoft. Bränslets densitet, svavel- och syrehalt valdes för utvärdering av stoftutsläpp. Densiteten ansågs vara ett mått på andelen tunga fraktioner i bränslet. Tidigare studier påvisade att svavelhalten är starkt kopplad till stoftmängden i avgaserna. Samma växande samband som mellan stoft och densitet förväntades även med ökande svavelhalt. Däremot påstods ökad syrehalt i bränslet minska stoftutsläpp. Forskningen är enig om att ökad syrehalt hämmar stoftbildningen, även om de exakta mekanismerna är okända.

Stoftmätningarna på CRU:n utfördes med tre olika system och tre olika bränslen, lätt brännolja, tung brännolja, och ett okänt dieselbränsle ämnat för bilar. Ifall en klar skillnad i stoftmassa mellan lätt och tung brännolja kunde observeras, kunde experimenten fortsättas med lätt brännolja med olika densitet, svavel- och syrehalt. Stoftmassan i avgaserna mättes med ELPI:n, trots att ELPI:n är bäst lämpad för mätning av partikelantal. Eftersom ELPI:n separerar partiklar enligt storlek studerades även massafördelningen av det insamlade stoftet.

Ingen av de tre systemen skapade repeterbara, tillförlitliga resultat. Eftersom skillnaden i massakoncentrationen var såpass liten mellan lätt och tung brännolja kunde inga slutsatser dras. Därmed förblev ändamålet obesvarat. Följande orsaker till de misslyckade mätningarna identifierades: termofores, sedimentering, elektrostatiska

[1] OJ L 252, 16.9.2016, s. 1

krafter, okontrollerad utspädning, otillräcklig provmängd och förluster p.g.a. partiklarnas tröghet.

En Wärtsilä W6L32 motor kördes med lätt brännolja och på 100 % last för att mäta massakoncentrationen stoft i avgaserna. ISO 9096 metoden användes parallellt med ELPI:n, vars avgasprov utspäddes i två omgångar tills utspädningsfaktorn var cirka 64 gånger. ELPI:n registrerade hälften av massakoncentrationen som uppmättes med ISO 9096 metoden. Orsaken ansågs vara den grundläggande skillnaden i mätmetoderna samt utspädningen före ELPI:n.

Ändamålet med motormätningarna var att uppskatta skillnaden mellan stoftmängden i avgaserna från CRU:n och en fullskalig (medelhastighets) dieselmotor. Resultaten från motorn och CRU:n konverterades till stoftmassa per injicerad bränsleenergi (mg/MJ). Det visade sig att motorns stoftutsläppt var lägre än CRU:ns. ISO 9096 metoden mätte 35 % och ELPI:n 67 % mindre stoft i motoravgaserna än vad som uppmättes på CRU:n med ELPI:n. Skillnaderna i utsläppen torde bero på motorns högre tryck och temperatur samt den sämre omblandningen av bränslet och syret i den statiska kammaren.

Möjligheten att utföra experiment på literskala är värdefull för fortsatta studier av dieselprocessen och stoftbildning. Förbättringsförslag för framtida mätsystem på CRU:n var att minimera antalet ventiler och skarpa hörn i avgasrören. Samtidigt borde avgasrören uppvärmas till en högre temperatur än för avgasen inuti. Ifall utspädning används är det nödvändigt att utföra dessa under kontrollerade omständigheter, både gällande utspädningsförhållandet och -temperaturen.

Acknowledgements

Behind all the tables and results in this master's thesis are a group of people whose names are not printed next to mine. Eirik Linde, for instance, answered my spontaneous phone call and trusted me to provide more insight into the issues on his desk. Further, a person who answered my questions open-mindedly, no matter how trivial, was Sofia Nystén. Tor Laurén from Åbo Akademi University, provided valuable feedback despite the distance between Vaasa and Turku.

Jens Sandelin and Tobias Eriksson introduced me to the art of particle measurements on the field. Their expertise is worth praising, and this thesis would not be half as exciting without their input. The team at the Fuel Laboratory provided me with the physical equipment needed to complete this work. They aided me with their input and camaraderie. Per Löfholm, thank you for your patience and trust in me.

Finally, I am grateful for the support, dinners and housing my family and relatives provided. An immense thanks to my boyfriend. Because of the above-mentioned persons, I can now call myself Master of Science in Technology.

Table of Contents

1. Introduction

Lately, diesel engines have been under scrutiny in the EU due to their particulate emissions. The focus has mainly concerned road vehicle engines, as they are the most visible representation of diesel engines in our everyday-life. However, the concern of particulate emissions involves also other fields, such as power generation and marine transport. This concern materialized in December 2017 when the European Commission published a new Best Available Technique Reference Document for Large Combustion Plants, aka. LCP BAT. Reaching the new emission limit on "dust" is mandatory for Wärtsilä, a manufacturer of diesel and gas engines for power generation and marine propulsion.

Particulate emissions are known as particles consisting of unburned char, tar, soot and ash particles among others. The definition of what particulates are, and what they consist of, varies with measurement method, and even then, the results are not definite. Engine exhaust particles exist in a wide range of sizes (10–1000 nm), some even below the detection limit of the most advanced measuring technology (Eastwood, 2008). Particulate restrictions are of importance, and not only because of the environmental implications of the particulate. Extensive studies show that particulates have serious health effects (Oberdörster et al., 2004).

The aim of this work was to measure how fuel properties influence particle mass concentration in a constant-volume chamber, a Combustion Research Unit (CRU) made by Fueltech. The aim was realized in pilot tests on the CRU. Furthermore, the pilot scale tests were compared to particulate emissions from a medium-speed diesel engine. Light fuel oil (LFO) is the main fuel considered throughout the work. Other fuels, such as heavy fuel oil (HFO), are included for contrasting purposes, or to support theory.

This work is divided into a literature section and an experimental section. The literature section presents the sources of particulate emissions in chapter *2*, and discusses the main particulate fractions in chapter *3*. Section *2.3.3* motivates the choice of fuel properties under study in this work. Findings from previous research are summarized in chapter *4*, which completes the literature section. The experimental section begins with

the CRU pilot measurements (chapter *4*), followed by the exhaust measurements on a large scale engine (chapter *6*). Further, the engine and CRU particle results are compared and discussed in chapter *7*. Finally, the conclusions are collected in chapter *8*.

1.1. Best Available Technique Document for Large Combustion Plants (LCP BAT)

The LCP BAT concerns all fuel-combusting installations with a total rated thermal input of 50 MW or more. The BAT uses the term “dust” for particulate emissions, and states that the dust from gas-oil combustion in diesel engines consists of soot and hydrocarbons (Lecomte et al., 2017). Primary control techniques for reducing particulate emissions can be divided into regular maintenance of combustion system (mainly updating injectors) and control of combustion parameters (Lecomte et al., 2017). These combustion parameters involve fuel atomisation quality, air-to-fuel ratio, and performance of equipment warming or pre-treating the fuel. Further, techniques for the prevention and control of dust and particle bound metals are fuel choice, electrostatic precipitators (ESP) and bag filters (Lecomte et al., 2017). Yearly and daily BAT-associated emission levels (AELs) of dust from existing HFO are 5–35 mg/ Nm^3 and 10–45 mg/ Nm^3 for gas-oil fired engines at 15 vol-% oxygen and standard conditions (Lecomte et al., 2017). For new installations, the levels are 5–10 mg/ Nm^3 and 10–20 mg/ Nm^3, yearly respectively daily (Lecomte et al., 2017). The new dust limit of 5–10 mg/Nm^3 must be met by all new power plants constructed in EU and countries applying European legislation.

1.2. Particulates Defined

Particulates are emitted by numerous sources from the wood-heated sauna to waste incineration plants. The mixture of particles and a gas is called an *aerosol*, of which chimney smoke is the classical example. The term *flue gas* is generally used for the released gases from a combustion plant. Meanwhile, *exhaust gases* are released by engines and this term will be applied in this work. *Particulate matter* signifies the solid and liquid matter in an aerosol, excluding the carrying medium. The acronym PM can indicate *particulate mass* as well as *particulate matter* in scientific literature. In this

work, PM means particulate mass. The chapter below discusses the definition of particulates in European standards and the size of particulates.

1.2.1. Standards

This part aims to enlighten how standards relevant in Europe define particulate matter. Most standards rely on the gravimetric method, i.e. mass of particulates collected on filter. After collection, the samples can be analysed to determine the chemical composition, for instance with thermal evaporation or solvent extraction. Also, real-time measurement methods are available. These utilize different properties of particulates to detect and/or quantify them. Further details of measurement methods can be found from the following sources: Giechaskiel et al. (2014), Eastwood (2008), and Hinds (1982).

The previously mentioned LCP BAT defines dust as particulate matter. A more detailed definition of particulates can be found in EN 13284-1 (Lecomte et al., 2017). EN 13284-1:2017 is a European standard for stationary source emissions for the determination of low range mass concentration of dust by gravimetric means. This standard is primarily developed for waste incineration plants but is also applicable to other stationary sources (EN13284-1:2017, 2017). EN 13284-1 defines dust as those particles dispersed at sampling conditions that can be collected on a filter (EN13284-1:2017, 2017). But the definition also specifies that dust is those particles remaining on the filter after drying (160 °C for a minimum of 1 h) (EN13284-1:2017, 2017). By definition then, EN 13284-1 measures primarily solid particles, and those hydrates and volatiles that remain on the filter after drying.

The standard conditions are reference values for a dry gas at a pressure of 101.3 kPa and temperature of 273.15 K. However, the filtration temperature is either the stack temperature or higher than the recommended temperature of 160 °C. This standard avoids capturing of the volatile fraction in particles due to the drying following the sampling. It is recognized in the standard that particulates are not always thermally stable, i.e. changes from particulate to gaseous form depending on the temperature and influence the results. When these variations in measurements occur, the highest temperature sustained by the sampling dust must be reported as well. Further, Annex

H states that a temperature suitable for all cases is not possible to define. The conventional filtration temperature of 160°C avoids collection of most volatile compounds and decomposes most hydrates (EN13284-1:2017, 2017). According to EN13284-1, the purpose with neglecting the volatile fraction is to obtain reproducible results.

EN 13284-1 is closely related to ISO 9096:2017 (E). ISO 9096 concerns stationary source emissions and their manual determination of PM concentration. According to ISO 9096 PM and dust are those particles dispersed in the gas phase under sampling conditions (ISO 9096:2017 (E), 2017). An additional note explains that everything collected on and upstream of the filter and remains on the filter after drying is considered PM, or dust. However, for some national standards, the definition of PM can be extended to condensables (volatiles) or reaction products. The standard conditions are the same in ISO 9096 as for EN 13284-1.

1.2.2. Particle Size

Particulates can be roughly divided into three categories: coarse mode, accumulation mode, and nucleation mode. The coarse mode particles are formed from particles in the accumulation mode. The particles have attached to the cylinder and exhaust system surfaces and then merged together (Kittelson, 1998). The coarse emissions are inconsistent and most likely comprise of a solid core and an outer layer of volatile material (Eastwood, 2008). The size of these particles is large enough, >2 µm in diameter, to entail even rust and scale from the exhaust system (Eastwood, 2008; Hinds, 1982).

Accumulation mode particles have received the greatest attention in scientific studies. They consist of a collection of smaller particles, called spherules[2]. The typical size range of spherules is 20–50 nm and they agglomerate to form more stable accumulation mode particles (Andreae & Gelencsér, 2006; Eastwood, 2008; Warnatz, Dibble, & Maas, 2006).

[2] Spherules differ from coke particles. Spherules are pyrolysis products of gaseous fuels, or volatilized intermediates of liquid or solid fuels. Coke particles are considerably greater in size, 1-50µm, and form through liquid-phase pyrolysis of fuel droplets, such as HFO (Eastwood, 2008; Glassman & Yetter, 2008).

The mean diameter of accumulation mode particles from vehicles is 60–100 nm (Burtscher, 2005). There is no defined morphology, everything from chains, clusters and rings have been observed (Eastwood, 2008; Heywood, 1988). Accumulation mode particles tend to acquire a liquid or viscid coating (Eastwood, 2008). For automotive emissions, most of the mass, between 60–96 % of particles, lies in the accumulation mode, while 5–20 % of the mass lies in the coarse mode particles (Kittelson, 1998).

The nucleation mode particles lie at the detection limit of many instruments (Eastwood, 2008). These particles consist of volatile material and thus are often depicted as spherical (Eastwood, 2008). The volatile material, consisting of organic and sulphur compounds, condenses during exhaust dilution and cooling to form liquid droplets (Kittelson, 1998). Research indicates that the nucleation mode particles may also contain solid compounds of carbon or metals, around which the volatiles condense (Eastwood, 2008; Kittelson, 1998). A typical size range for nucleation mode particles is 0.005–0.05 µm (5–50 nm) (Kittelson, 1998).

Particulate size is of relevance because it is connected to the health hazards. Typically, as particle size decreases the number of particles (PN) and the surface area per unit mass increases (Kittelson, 1998). A larger surface area makes the particulates more prone to absorbing potentially carcinogenic volatile matter. In fact, nucleation mode particles are typically > 90 % of PN, see Figure 1. What raises concerns is that pulmonary deposits increase with decreasing size (Oberdörster et al., 2004).

Currently, the aim of the legislation is to lower the mass of particulates, which does not prevent hazardous particulates from being released in the form of smaller particles (Kittelson, 1998). Regulation (EU) 2016/1628 of the European Parliament and of the Council of 14 September 2016 on requirements relating to gaseous and particulate pollutant emission limits and type-approval for internal combustion engines for non-road mobile machinery[3] have defined a PN limit (1×10^{12} /kWh) for engines on inland waterways vessels (European Parliament & Council of the European Union, 2016). However, this development has not yet been implemented for stationary engines, and

[3] OJ L 252, 16.9.2016, p. 1

for a few reasons. PN measurements have deficient repeatability, high uncertainty, and the measurement method is better suited for smaller engines.

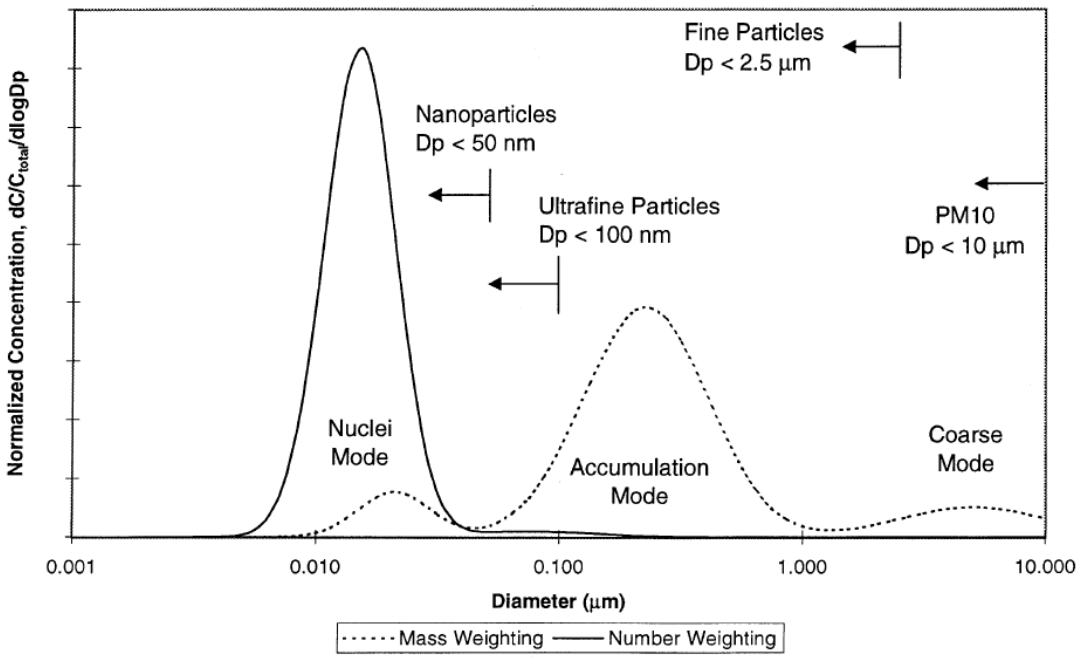

Figure 1. Lognormal mass and number weighting of different particulate modes (Kittelson, 1998).

2. Sources of Particulate Emissions

The combustion, rather than the engine, is under focus in the thesis. Consequently, the first section will shortly review the working principle of the diesel engine, and then describe the stages of combustion and engine parameters that influence particulate emissions. A brief section describes the use, composition and behaviour of lubrication oil in the engine. The last section concerns the fuel, of which both chemical and physical properties are covered. As the scope of this work is fuel properties, the fuel characteristics of interest are collected in section *2.3.3*.

2.1. Engine

2.1.1. Operating Principle of Diesel Engines

A diesel engine, a.k.a. compression-ignition (CI) engine, ignites fuel by pressure alone while a spark ignited engine uses a spark plug to initiate combustion. Applications vary from vehicles, locomotives, ships to power production. There are several categories of diesel engines, but the perhaps the most defining characteristics is whether the engine power cycle is done in two or four strokes. The 2-stroke engine operates on less revolutions per minute than the 4-stroke, and hence the names low-speed respectively medium-speed engine are also used. Wärtsilä produces only large four-stroke engines, or medium-speed engines.

The cycle begins with the *intake stroke* when the piston moves from its highest position, top-dead-centre (TDC), to its lowest (bottom-dead-centre, BCD) and draws in air (Heywood, 1988). The *compression stroke* presses the air into a smaller volume, which increases the pressure in the cylinder. Consequently, the temperature increases and before the end of the compression stroke the fuel is injected. Due to the high temperature the fuel droplets evaporate. Ignition occurs when the piston approaches TDC and the mixture reaches the ignition temperature of the fuel. The hot and high-pressure gases expand and press the piston from TDC to BDC, generating the *power stroke*. Before the piston reaches BDC, the exhaust valve opens, which lowers the pressure in the cylinder. Finally, the *exhaust stroke* results in the exhaust gases flowing out, both due to the pressure difference between the cylinder and the exhaust pipe, and

due to the upward movement of the piston. Air is introduced before TDC while the exhaust valve closes after TDC. Thus, the cycle starts again with the intake stroke.

Further, engines are categorized according to their air-intake method. Three configurations are possible: naturally aspirated, turbocharged, supercharged (Heywood, 1988). Natural aspiration inducts atmospheric air into the cylinder, while turbo- and supercharged engines induct compressed air. The main difference between a turbocharged and a supercharged engine is the method with which they generate compressed air. A supercharger compresses the air by a mechanically driven pump or blower. In contrast, a turbocharger is a combination of a turbine and a compressor. The turbine is driven by the engine exhaust gases, and the work from the turbine is transferred to the compressor. All Wärtsilä engines are turbocharged. The advantages are a higher power-weight ratio, reduced exhaust gas temperatures, and elimination of an external power source for compression. Induction of compressed air is advantageous because the density of input air increases, hence more air is delivered into the cylinder, the combustion is more complete, and thus more power is produced.

Engines can also be divided into direct-injected and indirect-injected engines. As the name indicates, direct-injected engines introduce the fuel into the cylinder immediately (Heywood, 1988). In contrast, engines with indirect- injection inject the fuel into an auxiliary combustion chamber above the piston. Combustion begins in the pre-chamber and when the pressure increases a mixture of fuel, burning gases and air are forced into the cylinder. Wärtsilä builds its engines solely with direct-injection.

2.1.2. Stages of Combustion

Engines operate in predefined cycles, and the time available for combustion is thus constrained. Naturally, this leaves a limited time for the fuel-air mixture to burn and produce work. In this short time-span, four distinct combustion phases can be identified (*Figure 2*): ignition delay, premixed phase, mixing-controlled phase (indicated as “rate-controlled combustion” in *Figure 2*), and late combustion (Wright, 2000).

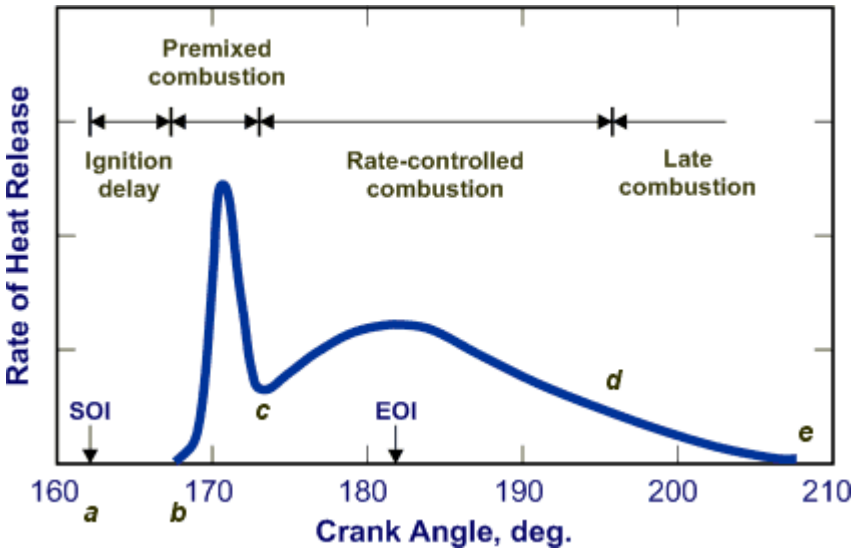

Figure 2. Heat release rate during combustion (Jääskeläinen & Khair, 2017).

Before the cylinder reaches TDC (180^{o} in *Figure 2*) the fuel spray is injected. As can be seen in *Figure 2*, a brief period separates the start of injection and start of combustion. This period is called *injection delay* (ID). During the span of a few milliseconds, the fuel blends with air to its flammable limits. The fuel is both physically and chemically modified during the ignition delay. Due to the pressure difference between the injection nozzle and the cylinder, the liquid fuel forms an atomized spray, which vaporises and mixes with air. A correct fuel viscosity is important for proper mixing. High-viscosity fuel forms large droplets, which can attach to the cylinder walls. In contrast, a low-viscosity fuel results in insufficient spray penetration. Engine-related parameters that influence the ignition delay are injection timing, charge air pressure and temperature, unit fuel charge, and oxygen concentration (Wright, 2000). Ignition delay is connected to the cetane number (see chapter *2.3.2*), or autoignition. The vapour phases of the fuel oxidize spontaneously. Simultaneously, larger hydrocarbons split to smaller compounds, which then oxidize. The molecular structure of the fuel influences the extent of "cracking", i.e. the fragmentation of heavy molecules. Aromatics, known for their stability, resist cracking and hence are associated with long ignition delay.

Because of the ignition delay, most of the already injected and mixed fuel combusts in the *premixed phase*. The injection has not yet stopped, and the fresh fuel burns together with the previously injected fuel. Consequently, the extensive heat release increases

cylinder pressure and temperature. The pressure wave that follows the ignition creates new combustion sites. A longer ignition delay ensures that more fuel is present when ignition occurs, which causes a higher peak pressure and temperature than with a short ignition delay. However, a too long ignition delay, and the consequent rapid pressure increase, can damage bearings and bypass piston rings.

The maximum heat release is achieved in the *mixing-controlled combustion phase*, also known as *diffusion combustion*. If the premixed phase was strong, then only a minor secondary peak is seen. The mixture formed during ignition delay is consumed. The burning rate is controlled by the rate at which still unburnt, recently injected fuel blends with air, i.e. heat released is directly proportional to mixing rate. More than 75 % of fuel is combusted in this stage (Heywood, 1988).

Finally, in the *late combustion phase* the remaining fuel burns well into the expansion stroke. Soot and fuel-rich combustion products are released (Heywood, 1988). The remaining, still-burning fuel is left either because the lastly injected fuel did not have time to react completely, or the combustion reactions were slow. Slow reaction rates are especially promoted towards the end of the combustion, when intermediate reaction products are diluted by exhaust gases. As the expansion stroke continues, temperature declines and consequently, kinetics slow until the reactions stop.

2.1.3. Engine Parameters and PM

The tuning opportunities of an engine are numerous. Therefore, this section will only introduce the most common engine parameters that influence particle formation. Diesel engines operate in excess oxygen (lean combustion), and thus the overall fuel-air ratio is not discussed here.

In power generation applications the engine is connected to a generator. The generator applies a resistance on the engine, which creates a force the engine works against. This resistance is also known as load or brake. In diesel engines, the load is controlled by the amount of fuel injected. More fuel in the cylinder results in higher pressure, and thus more work delivered by the engine. Engine load is studied to influence the formation of PM. The general perception is that PM emissions increase with decreasing load. Mostly,

high load is translated to an elevated temperature in the cylinder, and therefore a more complete combustion of the fuel. Sarvi and Zevenhoven (2010) reported that PM increased with decreasing load with LFO, while the opposite trend was seen with HFO. But studies exist where no relationship could be found between PM concentration and load. For instance, Anderson et al. (2015) measured PM on a marine engine at low load (<35 %) and found no correlation between load and PM concentration of distillate fuels. The theory in the study was that the common rail system, and the subsequent high injection pressure, influenced the PM trend.

Injection timing marks the crank-angle at which combustion starts. A general rule is that a retarded injection timing, i.e. fuel is injected closer to TDC, increases (smoke and) particulate emissions (Heywood, 1988). However, specific trends vary with engine design and types. The closer the injection is to TDC, the less time fuel has to mix, and more intermediate combustion products, among those soot particles, are formed. But retarded injection results in less NOx emissions, and thus opposes the requirement for low particle emissions (Sarvi & Zevenhoven, 2010)

Further, other characteristics of fuel injection, such as fuel nozzle design, fuel injection rate and pressure, are of importance because they define the spray formation and the air-fuel mixing. A study on injection parameters of large-scale diesel engines concluded that a high injection pressure improved both specific fuel consumption and soot formation (Sarvi & Zevenhoven, 2010). A high injection pressure enhances fuel atomisation, and consequently more lean burning areas are formed. Further, it was concluded that hydrocarbon emissions were more sensitive to mixing than to the temperature, and therefore injection nozzle design had more weight than injection timing. Moreover, fuel injection rate, i.e. amount of fuel per crank angle degrees, influences particulate formation. A higher injection rate increases fuel-air mixing which in turn reduces smoke or particulate emissions (Heywood, 1988). Due to the better mixing, the heat release rate increases, and NOx emissions are promoted.

2.2. Lubrication Oil

The purpose of the lubrication oil is to reduce the friction of the engine to enable the highest mechanical efficiency. Other functions include protection of surfaces against wear, heat dissipation from the piston and removal of harmful substances from cylinder walls. Moreover, the oil should not leak into the combustion chamber, which inevitably occurs.

Tornehed (2010) summarized in his dissertation the sources of lubrication oil in diesel engines as follows: turbo charger, valve stem seals, crank case ventilation and the cylinder system. The cylinder system was considered the principal contributor to oil-related particles. Four pathways for oil to be introduced to the cylinder were identified: throw-off, reverse blow-by, evaporation from cylinder walls, and top-land scraping (Tornehed, 2010). Oil driven upwards to the combustion area by inertial forces is called *throw-off*, while *reverse blow-by* is oil carried by gas past the piston ring. Remaining oil can also be scraped off the cylinder wall by the top land of the piston, or by deposits on the top land.

Lubrication oils are customized with base oil selection and additive packages to meet several criteria, e.g. oxidation stability, detergency, wear reduction properties and viscosity (Heywood, 1988). The importance of the additives is highlighted by the amount. According to internal data, c.a. 15–25 % of the oil is added components, while the base oil composes 75–85 % of the lubrication oil. Base oil consists mainly of saturated hydrocarbons, such as linear-, branched-, and cycloalkanes, with carbon number ranging between C_{18}–C_{25} (Kupareva et al., 2012; Liang et al., 2018). To enhance the properties of the base oil, detergents, antioxidants, viscosity improvers, corrosion inhibitors etc., are added. Reasonably, the additives contain both organic and inorganic elements. Sulphur is one component often used to measure the presence of oil in particles, as oil contains calcium and zinc sulphates ($CaSO_4$, $ZnSO_4$). Both calcium and zinc are frequently encountered in lubrication oil, calcium as a sulphur neutralizer and connected to base number (BN). Zinc is commonly present as zinc dialkyl dithiophosphate, an effective antioxidant (Kupareva et al., 2012). Phosphorus and silica are other common elements in additives, in antiwear respectively antifoaming agents.

Generally, amines act as multipurpose additives against oxidation and corrosion. Sulphonates, phenates, and carboxylates are present as detergents due to their polar functional group. Sterically hindered phenols are used as antioxidants.

Oil-related particles are often considered volatile, but studies indicate lubrication oil contributes also to the solid fraction of particles. Tornehed (2010) concluded that lubrication oil is the dominant source of ash emissions in heavy-duty engines.

Moreover, an Euro 5-compliant heavy-duty diesel engine, was estimated to emit 0.4–1.1 mg/kWh oil-originating carbon particles (Tornehed, 2010). A study measuring particles from oil in a modified diesel engine by using hydrogen as fuel, discovered that without soot from fuel, elemental carbon (EC) emissions still existed, and that EC mass increased when load was increased (Miller, Stipe, Habjan, & Ahlstrand, 2007). Both studies indicated that engine load influences the mass of oil-related particles; a higher load combusts the hydrocarbons in oil completely, which generates ash particles. In contrast, when the load is low, and thus also the temperature, oil escapes combustion and is released as intermediate combustion products.

2.3. Fuel

As previously stated, the focus of this thesis is on diesel fuels, or more distinctly, light fuel oil (LFO). The definition is necessary because power plants can operate on residual oils, i.e. the residuals from distillation that did not separate further. This viscous fuel, a.k.a. heavy fuel oil (HFO), is low in cost, but high in sulphur and ash content among others. Particulate emissions are high, and too far from the updated PM limit (within EU) to be accessible without extensive exhaust gas cleaning. Power plant engines can also operate on LFO, but due to the high fuel cost operating hours are kept to a minimum.

Crude oil consists to a considerable extent of various hydrocarbons (alkanes, cycloalkanes, polycyclic aromatics) and hetero-compounds containing nitrogen, oxygen, sulphur and metals, see Table 1 for the elemental composition of crude oil. The most frequently occurring metals in crude oil are nickel, iron and vanadium (Moulijn, Makkee, & van Diepen, 2013). The linear compounds are desirable for diesel fuel. *Gas oil* belongs

to the middle distillates from the refinery and is used both for diesel and light fuel oil. The difference between diesel and LFO is essentially their purpose. LFO is aimed for heating, low and medium-speed engines (both marine propulsion and power generation). Besides, diesel has more stringent quality restrictions than LFO, however the qualities are similar enough that LFO is suitable for cars.

Table 1. Elemental composition of crude oil (Moulijn et al., 2013)

Element	**Wt-%**
Carbon	83–87
Hydrogen	10–14
Nitrogen	0.2–3
Oxygen	0.05–1.5
Sulphur	0.05–6
Trace metals	< 0.1

2.3.1. Chemical Properties

Chemical properties are linked to molecular structure of the fuel, and thus the reaction pathways the fuel takes; either the pyrolytic reaction to soot or the oxidation to CO_2 and H_2O (Eastwood, 2008). The following section will discuss how the hydrocarbons present in the diesel influence particle formation. Also the oxygen and the sulphur content, and the inorganic compounds are presented in this framework. The terms ash and inorganic compounds are used interchangeably.

Hydrocarbons

Diesel fuel can roughly be said to contain 89 wt-% carbon and 14 wt-% hydrogen (Heywood, 1988). Diesel consists of various alkanes, naphthenes (ring-structures with single-bonds), alkenes, alkynes, aromatics and alcohols. These different hydrocarbons have different tendencies to form soot, and one could say that the quantity of carbonaceous particulates reflects the type of hydrocarbons present in the fuel (Eastwood, 2008).

Soot formation does not only depend on how the fuel molecules find oxygen, but also on the bonds in the molecules. Empirical observations note that for aliphatics the sooting tendency increases with molecule length, number of sidechains, and type of intermolecular bonds (i.e. single, double and triple bonds) (Eastwood, 2008). Alkenes generate generally more particulate, both organic and carbonaceous, than alkanes with the same carbon number. The double bond facilitates the formation of PAH. At high load the carbonaceous fraction increases, while at low load more organic particulates are generated. Aliphatics and their influence on soot formation seem to be partly connected to their boiling point, especially for alkanes. Further, carbon number remaining equal, saturated *rings* soot more than saturated *chains*. The more complex the molecule, the higher the likelihood for soot formation. The sooting tendency increases in the following order: alkanes, alkenes, alkynes, aromatics (Eastwood, 2008). However, Glassman & Yetter (2008) state that specific molecular structures do not play a role under premixed conditions. For instance, decane has the same sooting tendency as benzene at constant premixed flame temperature. Therefore, under premixed conditions, fuel molecules break down into the same species that form the soot particle. The principal compound contributing to soot particle growth is acetylene (Glassman & Yetter, 2008).

Aromatics are of concern for particulate emissions, because they are considered immediate soot precursors. Again, the correlation is not straightforward, and a few observations should be considered when studying aromatic-particulate correlations. First, particulate emissions depend on the engine, i.e. the combustion system and calibration (EGR, timing, injection pressure). Therefore, conditions might exist in the engine when air-fuel mixing is more important for soot than the chemical composition of the hydrocarbons present. Second, aromatics are tightly connected to other properties, such as cetane number, volatility, density, C/H-ratio. Third, both the organic and the carbonaceous fraction are influenced, and thus measuring total particulates is insufficient. Fuels with low aromatics content can reduce particulates through the organic fraction. This occurs because the absorption of the organic fraction onto the carbonaceous fraction is interrupted prematurely. Aromatic compounds with more rings are more important for soot formation than compounds with fewer. The current

understanding is that emitted PAH from engine are to a large degree escaped fuel compounds, and not pyrosynthesised intermediates. Following this logic, fuel formulation has a direct influence on particulate emissions.

Oxygen

As seen in Table 1, crude oil contains oxygen up to 1.5 wt-%. Not all oxygen is removed in the refinery process, however for ultra-low sulphur diesel (ULSD) this can occur (Moulijn et al., 2013). Remaining oxygen in the fuel or in additives (oxygenates) is present in alcohols, esters, ethers and carbonates. The primary target of oxygenates is soot. Two main theories for how fuel-oxygen reduces soot exist; either the oxygen discourages soot formation or encourages soot oxidation (Eastwood, 2008). The second theory proposes that oxygenates increase the concentration of CO and CO_2 or of OH. Meanwhile, the first theory suggests that carbon already bonded to oxygen is less prone to form soot due to the strength of the carbon-oxygen bond. But the nature of the carbon-oxygen bond is of importance. Carbonates and esters, which have the oxygen atom bonded to the same carbon atom, are less effective in soot-suppression than alcohols, which have the oxygen bonded to a single carbon atom (Eastwood, 2008).

Oxygenates are added on percentage level, and thus they also influence the physical properties of the fuel, such as density and viscosity. Especially at high oxygenate level, the reduced soot might not be due to the chemical properties. Instead the changed characteristics of the fuel spray, fuel flow characteristics and fuel atomisation affect the amount of soot. A study conducting autoignition tests in constant-volume chamber on diesel blends with ethanol and butanol confirmed that ignition delay increased with increasing alcohol content (Lapuerta, Hernández, Fernández-Rodríguez, & Cova-Bonillo, 2017). A long ignition delay means longer time for fuel-air mixing, and therefore less soot. The correlation between a long ignition delay and particle emissions is discussed in the next chapter (*2.3.2*). Large-scale measurements on a marine engine reported that the amount of black carbon was the lowest at all load points for a biodiesel blend[4]

[4] The blend consisted 70 % of marine diesel oil and 30 % of biodiesel. The biodiesel was a fatty acid-type component (Aakko-Saksa et al., 2016).

compared to distillate fuel and HFO (Aakko-Saksa et al., 2016). In the study the oxygen-content was considered the principal reason for the low amount of black carbon, which aligns with the theory that oxygenates target the carbonaceous fraction. But biodiesel was added to 30 %, which already alters the physical properties of the fuel.

Sulphur

Typical diesel fuel contains 0.1 to several wt-% sulphur (Sarvi, Fogelholm, & Zevenhoven, 2008). Crude oil contains naturally 0.05–6 wt-% sulphur which is removed either by hydrotreating or hydrocracking (Moulijn et al., 2013). Sulphur is infamous for its corrosion problems, due to its formation to sulphuric acid. In the exhaust stream sulphuric acid acts as a nucleating agent by promoting gas-to-particle conversion. Meanwhile in the dilution tunnel (in particulate measurements), the acid initiates the formation of secondary organic compounds. Therefore, it seems reasonable that less nanoparticles are emitted when the sulphuric acid content decreases in the exhaust.

Studies indicate that only 1–2 % of fuel-sulphur forms sulphate particulate (Sarvi et al., 2008). The remaining fuel-sulphur reacts to form gaseous sulphur dioxide (SO_2) and to a lesser extent sulphur trioxide (SO_3). Due to its gaseous form, SO_2 does not directly influence the amount of particulate. It is the hydrolysis of SO_3 that creates sulphuric acid (H_2SO_4) in the exhaust. Sulphuric acid is more active in influencing particles, for instance by initiating nucleation (Eastwood, 2008). Especially the organic fraction is susceptible to variations with sulphur content in the fuel. The effect is more prominent when particles are collected at low temperatures. Even though fuel-sulphur affects the total particle mass, sulphur appears to have negligible influence on the carbonaceous fraction (Aakko-Saksa et al., 2016; Sarvi, Lyyränen, Jokiniemi, & Zevenhoven, 2011). In warm sampling conditions, e.g. inside the stack at above 300 °C, sulphuric acid remains in gaseous phase, while metal sulphates might be present as solids (Aakko-Saksa et al., 2018).

However, the connection between sulphur content and particulates is slightly ambiguous, as the desulphurisation process alters the hydrocarbon speciation, particularly aromatics, which in turn is reflected in the burning characteristics

(Eastwood, 2008). Sulphur compounds tend to occupy the back-end of the distillation curve, and hence there is a vague correlation between fuel-sulphur and volatility.

Inorganics

The inorganic fraction, or commonly known as ash, can contain for instance calcium, zinc, magnesium, iron, copper, chromium, phosphorus, silicon, sulphur and aluminium (Heywood, 1988; Sarvi et al., 2011). The crude oil naturally contains these elements, and despite excessive processing not all of them are completely removed. Which elements are present in particles depends mostly on the fuel and lubrication oil composition (Sarvi et al., 2011). These elements can be atomically dispersed or present in nanodomains within the spherules, or attached to the spherules (Eastwood, 2008). Some studies suggest that these ash components are the kernel within primary particles, the stage before nucleation mode (Kittelson, 1998; Lyyränen, Jokiniemi, Kauppinen, & Joutsensaari, 1999). The ash content, of both fuels and particles, is traditionally defined by controllably combusting the fuel in an oven until only the ash remains. Ash in LFO is typically specified as below 0.01 wt-%. More precise values are rarely reported. Specific metals are generally reported to be below 1 mg/kg. One reason for this could be the uncertainty of the analysis.

2.3.2. Physical Properties

Physical properties control spray characteristics of the fuel. How well the fuel mixes with air is influenced by parameters such as cone angle and size of droplets. The chemical and physical properties are inherently related, and difficult to detach from each other. Similarly, various physical properties themselves are entwined with each other.

Volatility

For fuels volatility is reported with distillation curves. The distillation process separates hydrocarbons in the crude oil according to their boiling point. Also T10 (front-end) and T90 (back-end) temperatures are commonly reported in fuel analyses. T10 and T90 signify the temperature at which 10 % respectively 90 % of the fuel has evaporated. Typically, the T10 and T90 of the vehicle diesel are 180 °C respectively 320 $^{\circ}C$ (Eastwood, 2008). According to an undisclosed source, T10 and T90 for LFO can be approximately

230 respectively 360 °C. Betts, Fløysand & Kvinge (1992) considered the higher distillation point (T95) to be relevant for particulate emissions. Generally it is considered that when the high-boiling point fraction is low, less PM emissions are formed (Sarvi et al., 2008). Heavy molecules prevent the atomization of the fuel and thus cause more particulates. However, the explanation is not so straightforward, as also PAH and sulphur compounds are found in the back-end fraction, and they are notoriously noted for their participation in particulate formation (Eastwood, 2008; Karila et al., 2004).

The mixing of air and fuel causes two types of organic particles to form: direct and indirect (Eastwood, 2008). Direct organic particles are those hydrocarbons that escape combustion, while indirect organic particles are intermediates in soot-forming reactions. Low-volatile fuel, i.e. the back-end fraction, tends to *undermix*, which causes rich, soot-generating pockets to occur in the cylinder. Consequently, indirect organic particles are emitted. If the fuel droplets last longer in the cylinder, also direct organic particles are emitted. In contrast, the volatile fraction, i.e. front-end, runs the risk of *overmixing*, and fuel molecules struggle to find oxygen molecules to react with. Direct organic particles leave the cylinder when overmixing occurs.

Density

The density of LFO varies between 0.8–0.9 kg/L. A high-density fuel generates more particles, especially carbonaceous ones. Density influences the mass of fuel injected, because the injection is controlled by pulse widths, and thus is also volumetrically controlled (Kalghatgi, 2014). However, the mass of fuel injected is tied to engine parameters, such as ignition timing and EGR, and to other physical and chemical properties of the fuel. Engines are designed for a fuel with a certain density, to optimize fuel metering among others. Westerholm & Egebäck (1994) deduced that density was one fuel parameter of importance for emissions for light- and heavy-duty vehicles. Betts, Fløysand & Kvinge (1992) claimed that in European vehicles density had the strongest influence on particulates and that a linear correlation existed between these two. The relationship became non-linear at high densities (> 0.86 kg/L) due to over-fuelling with a notable growth in particulates and hydrocarbon emissions. But common-rail injectors, electrically controlled injectors, are standard equipment in light-duty vehicles, and

might influence the observations above. Wärtsilä engines in power production applications do not usually operate with common-rail injectors, but the trend is slowly changing. The advantages of the common-rail are that the injection rate and timing can be controlled (Jääskeläinen & Khair, 2015).

Cetane number (CN)

The CN of commercial diesel fuel varies between 40–55, while gas oil from hydrocracking have a CN up to 55–60 (Heywood, 1988; Moulijn et al., 2013). Shortly, the lower the CN of a fuel, the easier it is to ignite. CN is a measure of ignition delay and therefore also an indicator of the relative proportions of premixed and mixing-controlled combustion. The mixing-controlled combustion is the main reason for soot (Eastwood, 2008). Hence, a long ignition delay, i.e. low CN, is beneficial. But when the ignition delay is long, the fuel can overmix, collide with the cylinder wall or be absorbed onto the engine deposits, which shelter hydrocarbons from combustion and thus promote the release of organic particulates. CN depends on the molecular structure of the fuel (Heywood, 1988). Alkanes have a short ignition delay, and the delay grows with chain length. In contrast, alcohols, cycloalkanes, and aromatic compounds have a long ignition delay. Depending on the number of branches, iso-alkanes degrade the CN, unless the branches are at the end of the chain when they improve it.

A study measuring particles on medium-speed diesel engines found that upon comparing LFO and HFO, the emissions of hydrocarbons increased with increasing CN (Sarvi et al., 2008). The same study concluded that more particle mass was measured when CN was low, due to the reduced ignition delay and the importance of pre-mixed fuel combustion. Also Cowley, Stradling & Doyon (1993) and Fløysand & Kvinge (1992) thought CN to be relevant for particulates from light- and heavy-duty vehicles.

2.3.3. Fuel Properties of Study

This chapter has illustrated the complexity of diesel fuel and how inherently related fuel properties are. The aspects this work focuses on are density, sulphur content and oxygen content. A high density indicates of heavy molecules present from the back-end of the distillation curve. Thus more PM are expected with increasing density. LFO does not

contain sulphur to the same extent as HFO, but due to its strong influence on PM at all sampling temperatures it is motivated to investigate sulphur content in LFO. Similarly as with density, a high sulphur content is predicted to result in higher PM. Oxygen content of LFO is also studied and the fuel is used as received. Only the total oxygen content is in focus. How the oxygen is present is outside the scope of this work. PM is predicted to decrease with increasing oxygen in the fuel.

3. Fractions in Particulates

The particulate composition can be divided into a volatile and a non-volatile fraction, or soluble and insoluble fraction (Eastwood, 2008). This dual naming arises from how the fractions are measured. In chapter *1.2.2*, it was mentioned that solid (coarse mode) particulates have a solid core with a liquid, or volatile, coating. The volatile coating is generally considered to consist of the sulphate, the nitrate and the organic fraction, while the solid core is considered to be the carbonaceous and inorganic fraction (Eastwood, 2008; Heywood, 1988). The current chapter will explore the chemical composition of the solid and soluble particulate fractions.

3.1. Inorganic Fraction

The inorganic, or ash fraction in particulates should mirror ash composition in fuel (see chapter *0*). As discussed in the previous chapter, also the lubrication oil adds inorganic components to particulates.

Additives containing halogens increase the likelihood of soot for all fuels under diffusion flame conditions (Glassman & Yetter, 2008). The halogen acts as a homogenous catalyst in the extraction of hydrogen from hydrocarbons and consequently cause more available carbon for soot. Bonczyk (1991) studied metals and organometallic compounds in premixed flames. It is reported that a metal's efficiency to affect soot formation depends almost solely on temperature and the metal atom's ionization potential (Bonczyk, 1991). Therefore, the most effective elements in soot reduction are alkaline earth metals in the increasing order calcium, strontium, barium (Glassman & Yetter, 2008). The metal additive reduces soot particle size but increases the number density, as the ion charge transfer reduces agglomeration. Particle burnup is enhanced at the right conditions, especially in diffusion flames because smaller particles must pass the flame front.

The catalytic effect of metals was suspected in HFO particulate when at 100 % load less carbon was present in the small particle fraction (0.2 µm) than in the large fraction (0.5 µm) (Sarvi et al., 2011). Simultaneously, the opposite trend was observed with iron and nickel, where both elements were more abundant in the small PM fraction than the

large particle fraction. The same study reported that elements from lubrication oil were found in the large particle fraction (0.5–1 μm), while species from the fuel were found in the finer fraction (0.2–0.5 μm) (Sarvi et al., 2011). This observation concerned only the distribution of (solid) inorganic components in particles. Also a study on black carbon from marine fuels encountered the effect of metals on carbon burnout. At 25 % load, the fuel with the highest metal and sulphur content produced less black carbon than a cleaner fuel, indicating that especially at low load (and cooler temperature) the catalytic function of metal species was enhanced (Aakko-Saksa et al., 2016). Meanwhile, the cleanest fuel and the biofuel-blend had the least black carbon at all load conditions.

Apart from catalytic effects, inorganic components can act as a nucleating agent for primary particles. Vanadium and nickel from HFO and high-ash fuel, zinc from the engine oil and aluminium and silicon from catalytic cracking processes were found in the centre of primary particles by Lyyränen et al. (1999). The elements can also be metal oxides, and, especially for residual oils, nickel oxide was believed to be the first inorganic species to form particles (Lyyränen et al., 1999).

3.2. Carbonaceous Fraction

There is considerable confusion when it comes to defining and naming the carbonaceous fraction. The most common one is “soot”, which can mean anything from the powder inside a chimney to solid carbon. Additionally, *elemental carbon* (EC) and *black carbon* (BC) are widely used in scientific literature. The term EC is used when a thermal determination has been done, and thus refers to the carbon fraction that is oxidized in an oxygen-containing environment above a certain temperature (Andreae & Gelencsér, 2006). Optical methods detect BC, which is considered the responsible component for the absorption of visible light (Andreae & Gelencsér, 2006).

What is meant with the term “carbonaceous” is the absence of any specific carbon compounds (Eastwood, 2008). Andreae & Gelencsér (2006) call the carbonaceous fraction *soot carbon* and defined it as aggregates of spherules consisting of graphene layers with smaller amounts of hetero atoms, especially oxygen and hydrogen, bound to the graphene. The definition of soot carbon stresses that organic substances

commonly encountered in combustion particles are not included (Andreae & Gelencsér, 2006).

In this work the term soot is used for the carbonaceous fraction and soot carbon. The structure of combustion soot spherules is highly dependent on the chemical and thermal environment of the combustion (Andreae & Gelencsér, 2006). Also the annealing time has a significant influence on the structure. When the spherules are formed rapidly the structure is almost amorphous, while under a slightly longer residence time in the combustion zone fullerenic structures develop. When the residence time is seconds to minutes, or the temperature is elevated, highly ordered carbon structures form in the spherules. The average elemental composition (by weight) of combustion particles are 85–95 % carbon, 3–8 % oxygen, and 1–3 % hydrogen (Andreae & Gelencsér, 2006). The combustion efficiency has an impact on the amount of attached oxygen on the spherules surface. The higher the efficiency, the higher the amount of oxygen bonded to the surface and the more amorphous the soot (Andreae & Gelencsér, 2006). Consequently, the chemical reactivity of soot increases.

A study on in-cylinder soot concluded that the relative amount of aliphatic C-H groups are more important for soot oxidation reactivity than oxygenated functional groups (C-OH and C=O groups) (Wang et al., 2013). Furthermore, the soot from diesel engines generally have a carbon-to-hydrogen mole ratio of 3–6, while the same ratio for carbon black is 8–20 (Andreae & Gelencsér, 2006). These added components cause soot to behave differently from graphite. Another study on particles from a light-duty diesel engine found that soot samples from high engine load (70–100 %) appeared to have a more graphitic structure, while at low load the particles seemed amorphous, with more soluble organic fractions (Lee, Zhu, Ciatti, Yozgatligil, & Choi, 2003). Based on the theory by Andreae & Gelencsér, the result by Lee at al. indicates the combustion efficiency for the light-duty engine in question was higher when engine load was below 70 %.

3.3. Organic Fraction

The measurement method defines how the liquid fragment of particulates are named. Dissolution in an organic solvent, such as dichloromethane or a benzene-ethanol blend,

results in the extraction of the soluble organic fraction (SOF) from the solids (Heywood, 1988). If the samples are heated, the volatile organic fraction (VOF) is separated. Usually, the mass of SOF equals the mass of VOF, however their chemical compositions differ (Eastwood, 2008). The organic fraction of particulates was not analysed in this work. Therefore, this section will only briefly introduce the type of components contained in the named fraction.

The organic fraction, a.k.a. unburned hydrocarbons, is the most diverse part of the particulate composition. Everything from alkanes, alkenes, alcohols, esters, ketones, acids, ethers and aromatics can be present (Eastwood, 2008). The surface attraction is strong enough to attract normally gaseous compounds with four to eight carbon atoms (C_4–C_8) (Eastwood, 2008). The lubrication oil may contribute significantly to the organic fraction (Heywood, 1988).

The sulphate fraction is considered to originate from the fuel, especially for power generating diesel engines, as they may operate on heavy fuel oil (HFO) with high sulphur content. However, even if the fuel sulphur content is low, the burning of lubrication oil additives still causes sulphate emissions (Sarvi et al., 2011). Sulphate, or the SO_4^{2-}ion, is connected to sulphuric acid (H_2SO_4), a strongly water-associating compound (Eastwood, 2008). The association is so strong, that the water content of particulates correlates with the acid content.

Nitrate chemistry is extensively discussed in atmospheric literature. The most known example is nitric acid (HNO_3), the reason behind acid rain. However, nitrates are also found in the volatile fraction of particulates. The nitrate fraction denotes the water-soluble nitrates, i.e. the NO_3- ion, and nitric acid (HNO_3) (Eastwood, 2008). Nitric acid is the main component of this small fraction. The acid is a reaction product of water and NO_2, and thus connected to NOx chemistry. Studies indicate that the sulphate and nitrate precursors compete for exhaust gas oxygen, as opposite trends exist between sulphates and nitrates (Eastwood, 2008). However, nitrates are more volatile than their sulphuric counterparts (the boiling point of nitric acid is lower than that of sulphuric acid). Therefore, nitrates are less likely to condense in the exhaust system than sulphates.

4. Previous Research

Previous studies about particulate mass from a constant-volume chamber are scarce. The device used in this work, the Combustion Research Unit (CRU) manufactured by Fueltech, has similarities with the Ignition Quality Test (IQT). The IQT measures ignition delay, and subsequently determines the cetane number (CN) of a fuel. Also the IQT is performed in a temperature-controlled, constant-volume chamber, and reasonably, most studies available measure the autoignition quality of various fuels. One of the studies with the CRU is by Hu et al. (2013). They conducted experiments on *n*-heptane, as a surrogate for diesel fuel, to determine the influence of temperature and pressure on ignition delay (ID). Another study by Rabl et al. (2015) applied the CRU to determine the correlation between ID and burn rate of blends of heptamethylnonane and cetane. Ghojel & Tran (2010) used laser imaging of soot to study ignition and combustion properties of diesel-water emulsions, but unfortunately did not to determine the mass of particles formed.

The closest study found that aligned with the aim of this work is by Kook & Pickett (2011). They studied the soot volume fraction of jet fuel sprays by laser imaging. Additional samples were extracted with a thermophoretic probe and analysed by transmission electron microscopy (TEM). However, laser imaging does not provide quantitative emission results, and is thus difficult to compare with other studies. All in all, the aim of this work is of interest, because no other studies were found that measure quantitatively particulate mass from a constant-volume chamber of diesel fuel.

Studies comparing electrical low-pressure impactor (ELPI) by Dekati Ltd. and the ISO 9096 standard are more common. The main purpose of ELPI is to measure particle number and size distribution. However, through a few assumptions, the particle number recorded by ELPI can be converted to particle mass. ISO 9096 is a gravimetric method and thus measures mass of particles. A study conducted by Ushakov et al. (2013) used ELPI to assess the particle mass concentration of a heavy-duty diesel engine operating on marine gas oil. At full speed and a dilution temperature of 400 $^{\circ}\mathrm{C}$, the particle mass concentration varied between 3–13 mg/m^3 in load range of 8–60 %. Additionally, a study measuring particle mass with ISO 9096 was conducted by Aakko-Saksa et al. (2018). The

medium-speed marine engine (Wärtsilä Vasa 4R32 LN) and the particle mass concentration obtained at 75 % and 25 % load was 9.5 and 25.5 mg/Nm3 respectively with a fuel containing 0.1 wt-% sulphur.

5. Combustion Reaction Unit Tests

This chapter contains the obtained PM results from exhaust released from a Combustion Reaction Unit (CRU). The CRU is a constant-volume combustion chamber and used in the Fuel Laboratory at Wärtsilä to measure ignition delay of various fuels. Three setup versions and three different fuels are experimented with, namely LFO, HFO and a random vehicle diesel, see Table 2. Challenges in designing was caused by constraints from both ELPI and CRU. The setups are planned to our best knowledge and the first goal was to combine everything without compromising safety.

The aim with the tests were to compare LFO fuels and their dust emissions. In order to compare very similar fuels, the experiments were first conducted with LFO and HFO. These two fuels represent the worst respectively best fuel in terms of particulate emissions. If the difference in particulate release was repeatable and distinct enough, then various LFOs could be tested. This stage was not reached in this work. The chapter below will thus present the results from LFO, HFO and the car diesel used.

Table 2. Properties of LFO and HFO in CRU experiments

Property	**LFO**	**HFO**
Density (at 15 °C, kg/m3)	841	990
Viscosity (at 80 °C, mm2/s)	1.81	44.1
Water (% V/V)	< 0.01	0.01
Ash (% m/m)	< 0.010	0.038
Sulphur (mg/kg)	< 10	7100
Net Specific energy (MJ/ kg)	42.8	41.0
Calculated Cetane Index	56	-
Carbon (% m/m)	86.9	88.0
Hydrogen (% m/m)	13.7	10.4
Oxygen (% m/m)	<0.2	0.48

First, detailed information about the combustion chamber (CRU) and ELPI are provided. Then, the setup versions are explained, upon which the results are presented in the

following subchapter. Finally, the results and setups are discussed and evaluated in the end of this chapter.

5.1. Apparatus

5.1.1. Combustion Research Unit (CRU)

For a producer of large-bore engines, it is valuable to perform fuel tests on a small scale, as engine-scale test have high operating costs, partly due to the extensive fuel consumption. Another drawback with measuring particles emissions from an engine is that the influence of lubrication oil cannot be excluded. The Fuel Laboratory at Wärtsilä has a Combustion Reaction Unit, also known as CRU, which is a constant-volume combustion chamber. As no moving parts are involved, no lubrication oil is required.

CRU is used to measure the ignition delay of fuels by igniting fuels by pressure alone. The ca 0.5 L combustion chamber is filled with air to a desired pressure and temperature, after which the fuel is injected and combusted. The pressure development during combustion is measured, along with other parameters such as injection delay. CRU has not been used, nor intended for, for particle measurements. Hence, all systems are solely designed for these pilot particle tests. The advantage of the CRU is also its drawback; a single CRU combustion is hardly representative of a running engine with several cylinders. Therefore, the obtained results in this work are not directly comparable with a diesel engine.

The CRU was operated in two modes, differentiated by the initial chamber pressure and temperature. The modes are called low and high mode in this work. For low mode, the temperature of the air in the chamber is 550 °C and pressure is 55 bar, while the same parameters are 570 °C respectively 70 bar for high mode. Both modes were used in the experiments, however most experiments were executed on low mode. Otherwise, no parameters were changed, except the injection pressure (the pressure with which fuel is introduced to the chamber) was changed once to 700 bar. All other measurements were executed with the default injection pressure of 1000 bar.

5.1.2. Electrical Low-Pressure Impactor (ELPI)

An Electrical Low-Pressure Impactor (ELPI) by Dekati measures particle size distributions in real-time. Particles are charged with a corona charger and then classified in a low-pressure cascade impactor according to aerodynamic particle size (Dekati Ltd., 2016). Impactor stages record the acquired charge as particles land on them. The subsequent current is directly proportional to the number concentration for that impactor stage. Particles in the range 0.016 µm to 10 µm are divided into 13 size fractions and collected on aluminium foil (Dekati Ltd., 2016). The 14th stage is a back-up filter and covers the size range 6 nm to 16 nm.

As mentioned, ELPI records particle number, which can be converted to PM. Based on assumptions related to particle density, shape and aerodynamic diameter the mass was calculated. This method does not equal that of a standardised filter setup. Maricq, Xu & Chase (2006), claimed that the particle mass uncertainty by ELPI varies around 20 % from the actual mass. However, the uncertainty is systematic[5], which allows comparison of results. Actual values are hence advised to study with caution.

The most important conditions to enable normal ELPI operation are collected in *Table 3*. Electrometers in ELPI record signals every second (sampling rate) in a known air flow of 10 L/min. Further, the pressure under the first stage is 40 mbar and the gas introduced to ELPI should be below 60 °C.

Table 3. Operating conditions and criteria of ELPI (Dekati Ltd., 2016)

Property	
Sample gas temperature [°C]	< 60
Pressure (absolute) [mbar]	40
Nominal air flow [L/min]	10
Sampling rate [Hz]	10

[5] The uncertainty is caused by the error in the effective density of particles (Maricq et al., 2006).

5.2. Setup Versions

Particle emissions were measured with three distinctive setups. Version 1 collects four CRU combustions into an 8 L tank, upon which the exhaust is measured by ELPI. The reasoning behind collecting the exhaust was to ensure collection of enough exhaust to obtain a stable reading at ELPI. In addition, this setup minimized exhaust gas losses. The container was removed for version 2 and 3, and a smaller tank (ca. 0.5 L) at atmospheric pressure was used instead. The idea was to utilize a plug-flow concept, in which the high-pressure exhaust gas pushes out the air in the tank, and ELPI extracts a representative sample from the tank. Thus, in versions 2 and 3, ELPI measured CRU exhaust directly, while in version 1 an ELPI measurement was a collection of four CRU runs.

To enhance understanding a few, frequently used words are described here. A *set* is defined as a series of seven combustions (this is the standard number of combustions in CRU). In version 2 and 3 the exhaust gas of one CRU combustion is directly measured by ELPI. This is called a *measurement*. “Measurement” is also used in version 1, but one measurement by ELPI corresponds to four CRU combustions. PM stands for *particulate mass*.

5.2.1. Version 1

The first system that was tested for particle measurements can be seen in Figure 3 and *Figure 4*. Valves 8 and 9 were leftovers from the very first trials and were not removed because the contained the fittings for ELPI. For a detailed view of buffer tank A and B, see *Figure 19* respectively *Figure 20* in the appendix. The schematic view is seen in *Figure 3* and the actual setup is presented in *Figure 4*.

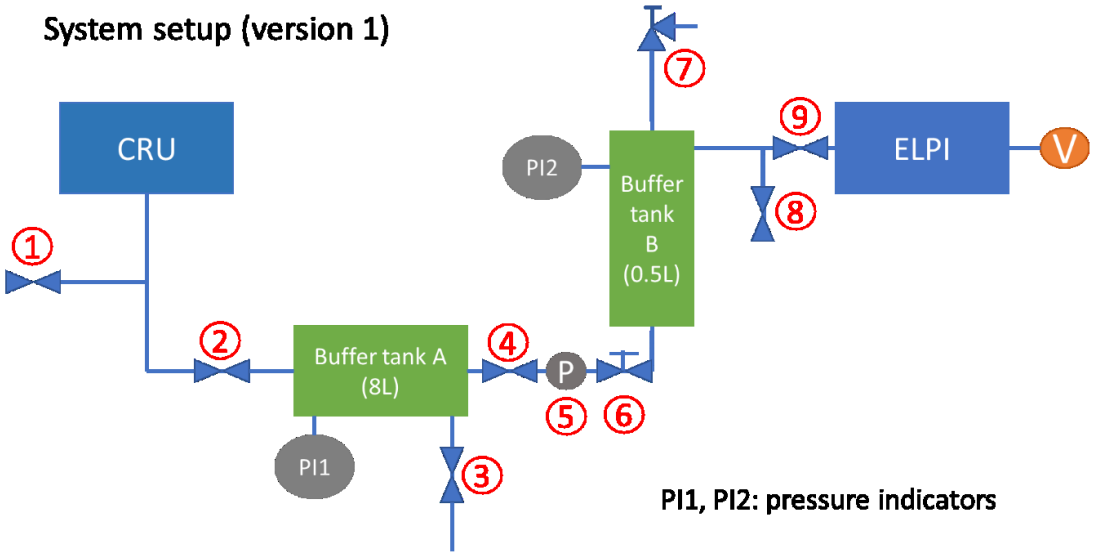

Figure 3. Schematic view of CRU-ELPI system, first version. Function of valves were as follows: 1) Opened for normal CRU operation, closed for loading buffer tank A. 2) Opened to fill buffer tank A. 3) Opened to flush tank A. 4) Opened to release exhaust gas into buffer tank B. 5) Pressure controller. 6) Flow control valve. 7) Pressure relief valve with an opening pressure of 1 bar. 8) Not used. 9) Release exhaust into ELPI.

Figure 4. Setup version 1. ELPI is not seen in the picture. The blue tank is buffer tank A. Buffer tank B is encircled.

System Operation

CRU operated on low mode, i.e. chamber conditions at fuel injection are: 55 bar and 550 °C. After complete CRU preparation (rinsing lines with sample fuel, calibration[6], heat-up etc.), the following were done:

Buffer tank A was vacuumed by ELPI until the pressure in it was stable (-0.95 bar (gauge)). This was only performed when the system had been inactive for a longer period, >1 hr.[7] Then valve 4 was closed to enable charging of exhaust into buffer tank A. The vacuumed buffer tank was rinsed two times with exhaust gases by opening valve 2 and 3. When the pressure reached ca. zero bar valve 3 was closed.

After the "rinsing procedure" of buffer tank A, four CRU runs were led into the same buffer tank by opening valve 2. In total, this lasted approximately 8 minutes until the buffer tank was filled, with a more exhaust introduced every 2 minutes. Depending on the initial pressure in the buffer tank, the final pressure before opening valve 4 to ELPI ranged between 5–5.55 bar. The pressure after each added exhaust charge was noted.

While the buffer tank was filled, the vacuum pump kept the system behind valve 4 at under-pressure. The measurement was started by opening valve 4, and the exhaust was released to buffer tank B. The pressure and flow controllers were adjusted to allow stable measurement conditions. The pressure in the buffer tank B was kept below 1 bar to avoid opening of pressure relief valve 7. Valve 4 was closed when pressure in buffer tank A reached ca. 0.5 bar. Valve 8 was always closed while valve 9 was always open. One ELPI measurement lasted approximately 4 minutes.

When the buffer tank A was empty of exhaust gases, valve 4 was closed. A new measurement was started by loading buffer tank A again.

---

[6] After CRU had calibrated itself, valve 1 was closed.

[7] The sealings were not completely tight, and leaked air.

5.2.2. Version 2

The results from version 1 indicate that particles accumulated somewhere (valves, inside of pipe walls). Based on this observation the setup was updated. Buffer tank A was removed, which left only buffer tank B for gas expansion, see *Figure 5*. Also the Teflon ducts were removed and the duct between buffer tank B and ELPI was changed to copper *Figure 6*. The pressure relief valve was also removed, but the casing was kept for the silencer (which added a negligible pressure on the inside). Lastly, a temperature sensor was installed before ELPI. Further, upon unscrewing parts from tank A, brown dust was visible. A thin layer of this same dust was found in the inside of ELPI cone. See appendices for microscope pictures of the dust.

With a smaller buffer tank, the exhaust gas would resemble more a plug-flow system. The drawback was that the ELPI intake was located at the top of buffer tank B, which made the system prone to uncontrolled dilution while measuring. An ELPI inlet at the bottom of the vertical buffer tank had been preferred, to minimise the content of air in the measured exhaust. Another predicted outcome was that the measurements would be completed faster. Further, the pressure increase when opening valve 2 might be higher and disrupt ELPI measurement for longer compared to version 1. Presumably, the first few seconds are the most representative (least dilution), before air enters buffer tank B again. The particle distribution should move towards smaller particle size in relation to version 1. To obtain repeatable results, operation of valve 2 should be defined (influences the gas flow, hence pressure and measurement duration).

Despite the mentioned disadvantages, the system was tested to verify that a direct measurement resulted in less particle interaction. The aim was to have an inert system that would not interact with particles during their way to ELPI. But most of all, the goal was to achieve repeatable results.

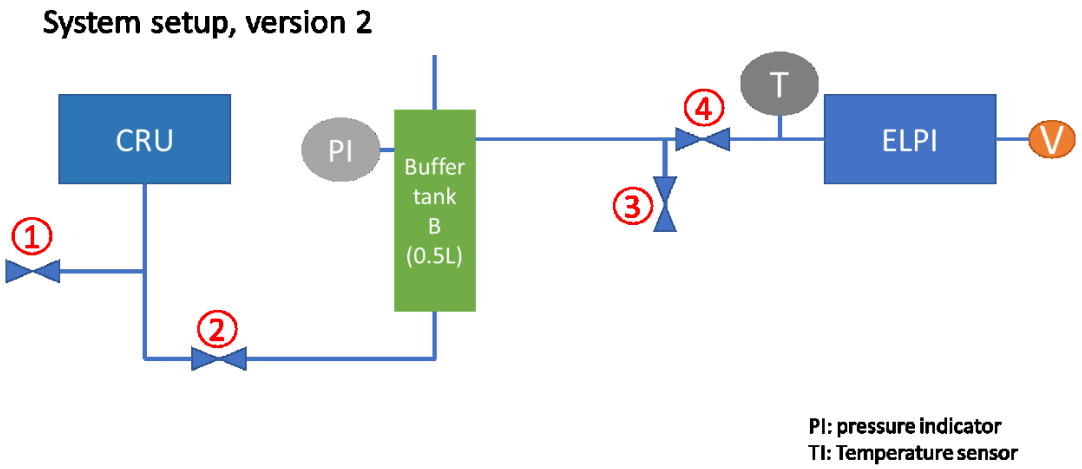

Figure 5. Schematic view of the second measurement setup. The function of valves was as follows: 1) Opened for normal CRU operation, closed for loading buffer tank B. 2) Opened to fill buffer tank B. 3) Not used. 4) Release exhaust into ELPI.

Figure 6. Setup version 2, with the installed copper duct connecting buffer tank B and ELPI.

System Operation

The experiments were performed at low mode, i.e. chamber conditions at fuel injection were 55 bar and 550 °C. CRU was prepared by rinsing lines with the sample fuel, airing pipes and by its self-calibration.

An ELPI measurement was begun by opening valve 2 when CRU combustion complete and closed again when the CRU air intake ticked. If valve 2 was closed too late, air was introduced to buffer tank B. Other valves were not operated actively during a measurement; valve 1 and 3 were closed, while valve 4 remained open. ELPI recorded the maximum current approximately few seconds after opening of valve. How much valve 2 is opened influenced the shape and height of the registered peak (property: current (fA)).

Pressure in ELPI was not disturbed when exhaust gas introduced to buffer B. Peak times were noted and an eye was kept on pressure in buffer tank B. However, the time when a peak was considered complete is inexact because ELPI current (fA) values dwindle. The time of completion was estimated from the timeline in ELPI during the measurement. Furthermore, no visible temperature peaks could be identified from the flow to ELPI. The temperature pulse was probably too fast for the probe to record.

5.2.3. Version 3

Only minor modifications were done on version 2 for the updated version, see *Figure 7* and *Figure 8*. The goal was to simplify operation and reduce particle diffusion to duct walls. In practice, this included installation of trace heating on ducts between CRU and ELPI, and installation of an on-off valve (3) before buffer tank B. What separates version 3 from its predecessor is the operating mode. All measurements in version 1 and 2 have been run in low mode. The hypothesis was that the difference in PM emissions from LFO and HFO would increase when CRU was operated on high mode. In the elevated pressure and temperature conditions, ash-related particles would be more prominent in exhaust from HFO than from LFO. The ash content in the HFO and LFO are 0.036 respectively < 0.01 %m/m. Heated lines would reduce particle losses by diffusion to the walls. However, due to a CRU malfunction, the time available for experiments was

significantly reduced. Consequently, measurements with activated heated lines were not performed. Problems with the CRU fuel injector prevented experiments with HFO on high mode from completion. No results are available from those measurements. Thus, only LFO results are presented in this chapter.

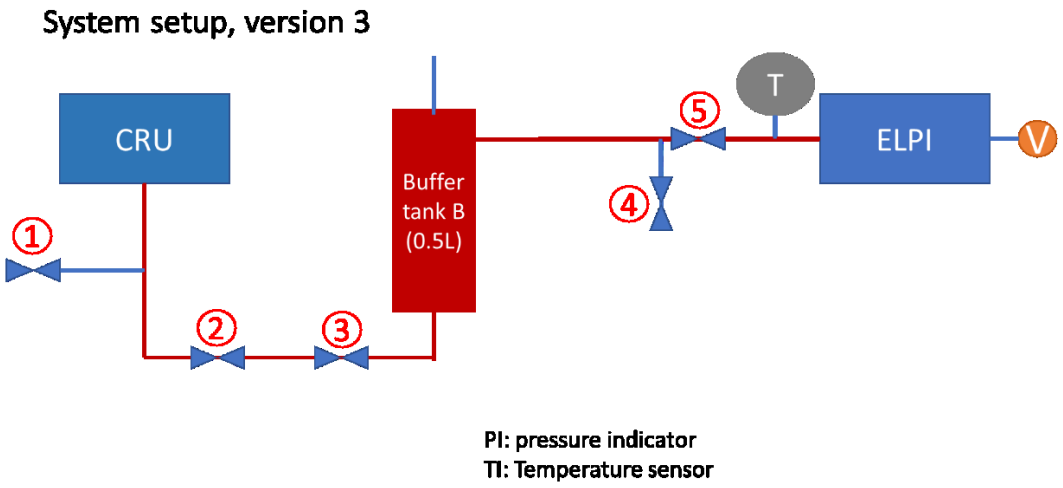

Figure 7. Schematic view of version 3. Function of valves are as follows: 1) Opened for normal CRU operation, closed for loading buffer tank B. 2) Open to fill buffer tank B. 3) On-off valve to regulate duration of measurement. 4) Not used. 5) Open to release exhaust into ELPI.

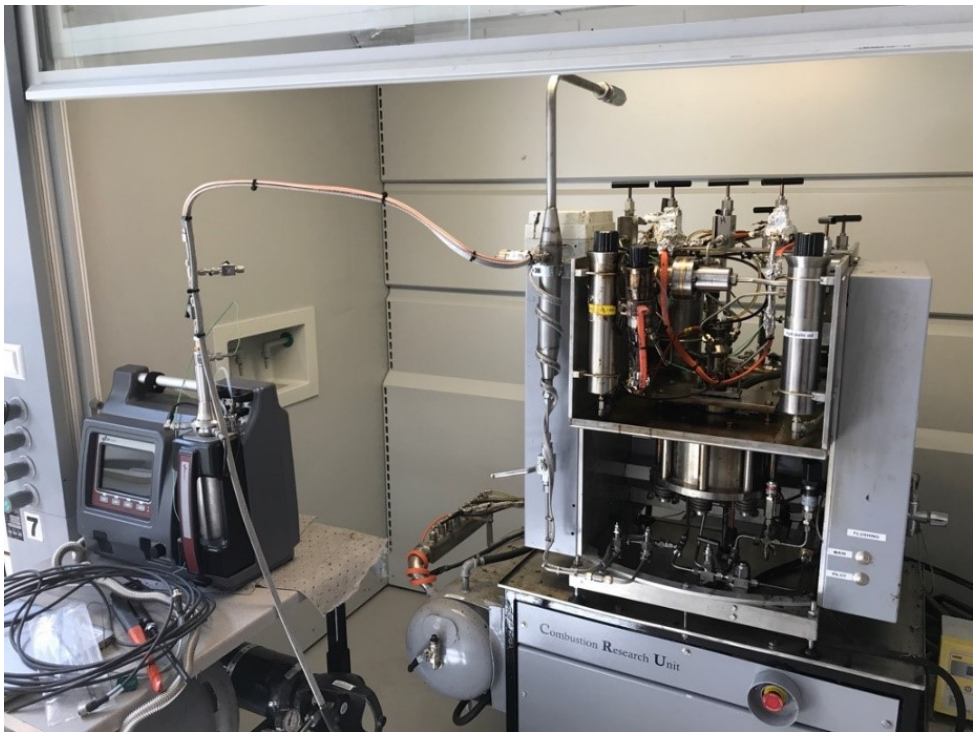

Figure 8. System update to version 3.

System Operation

As mentioned above, CRU was operated at high mode, i.e. chamber conditions at fuel injection were 70 bar and 590 °C. CRU was prepared by rinsing lines with the sample fuel, airing pipes and by its self-calibration.

An ELPI measurement was done similarly as in version 2. The first set, set 7a, was performed with valve 3 open and controlled with valve 2. The following two sets, 7b and 7c, were measured differently. After calibration valve 2 and 3 were opened. Only valve 3 was closed after 8 seconds when the CRU air-intake ticked. Approximately a 3 s delay existed between opening of valve 3 and first signal in ELPI. Furthermore, a minor pressure increase was noted in ELPI upon opening of valve 3. But the pressure returned rapidly to its original level. Again, ELPI peak times were noted.

5.3. Results

In this chapter, PM results and particle mass distributions from the three versions are presented. Recall that version 1 entailed two buffer tanks, A and B, and four CRU combustions were collected in buffer tank A before releasing them to ELPI. Meanwhile, in version 2 and 3 the exhaust gas was directly measured in atmospheric conditions from one smaller buffer tank (B). Further, the PM results were evaluated against two combustion parameters, namely ignition delay (ID) and maximum pressure increase (MPI). Ignition delay is the time between start of injection and start of combustion. The developed pressure in the chamber is indicated by *MPI*. The purpose of these parameters was to monitor the combustion behaviour and the consequent particle emissions. In most cases, MPI and ID of one version are not compared with each other or with other versions. Due to the outcome of the experiments, a detailed evaluation of combustion parameters on particulate emissions is not viable to make.

5.3.1. Version 1

Version 1 consisted of two buffer tanks and exhaust gases from four CRU combustions were measured by ELPI. ELPI measures particles as current per second (fA/s), and thus the timeline of the measurements was available. The mass per measurement was acquired from ELPI by selecting the time interval of the measurement. On average, the

measurements lasted approximately 4 minutes. Table 4 presents ELPI average PM concentration (average of 4–14 ELPI measurements) for the different fuels. Only stages 1–10 (size 0.01–1.2 µm) were included because ELPI frequently overestimates the presence of coarse mode particles. This inaccuracy originates from errors in the measured currents, such as electrical noise, electrometer drift, diffusion and corrections in electrostatic loss, which are enhanced when PM concentration is studied (Maricq et al., 2006).

Prior to fuel injection the chamber was filled with air. The heating coils around the chamber elevated the temperature of the air inside, which in turn increased the pressure. The CRU regulated the necessary amount of air required to reach desired conditions (temperature and pressure). Atmospheric air contains c.a 21 vol-% oxygen, and therefore the combustion was excessively lean. Considering the small amount of injected fuel (see chapter *7.1*), the oxygen content in the exhaust was assumed be reduced maximum by a few percent.

Table 4. Particulate emissions measured by ELPI, version 1

Campaign #	LFO PM (1–10) [mg/m3]	Car diesel PM (1–10) [mg/m3]	HFO PM (1–10) [mg/m3]
1	3.9 ± 0.5		7.5 ± 0.3
2	2.8 ± 0.6		3.3 ± 0.5
3		3.0 ± 0.5	
4	0.9 ± 0.1		

PM decreases over time, particularly seen in the LFO results with mass reduction of 1 mg/m^3 per campaign. A notable decrease (4.2 mg/m^3) is also observed for HFO between the particulate emissions of the first and the second campaign. Car diesel aligns with the early LFO emissions (campaign 1 and 2), which is expected due to their (presumed) similarity in fuel composition[8].

[8] The properties of the car diesel are unknown. It was assumed that car diesel is close to light fuel oil in composition and properties.

Table 5 presents selected CRU parameters: ignition delay (ID) and maximum pressure increase (MPI). What should be noted is the how constant both ID and MPI are within campaigns of the same fuel. Consequently, the decreasing PM is most likely due to the design, rather than fluctuations in CRU. The parameters for LFO and car diesel are identical, which suggests they are either similar in composition or that the difference is lost in the data processing.

HFO consist of heavier fractions and aromatics, than LFO, and as previously discussed in chapter *2.1.2*, aromatics tend to have a long ID. Assuming a constant amount of injected fuel, a high MPI is an indication of a more complete combustion. This is because more gaseous reaction products are formed the closer the combustion is to completion. In other words, the higher the pressure development (MPI), the more gaseous components have formed, which indicates fewer solid particles have been generated.

Table 5. Selected CRU combustion data, version 1

Fuel	ID [ms]	MPI [bar]
LFO 1	1.6	11
LFO 2	1.6	12
LFO 4	1.6	12
Car diesel 3	1.6	12
HFO 1	2.6	6.9
HFO 2	2.6	7.0

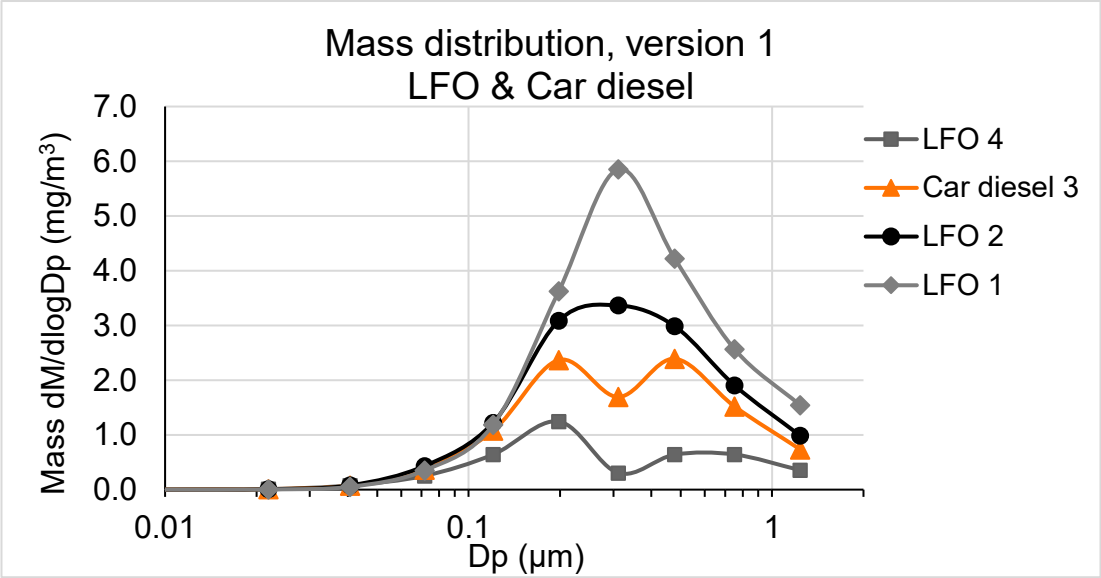

Figure 9. Mass distribution of LFO and car diesel, version 1. ELPI stages 1–10 are shown. The x-axis (D_p) is the aerodynamic particle diameter, and y-axis ($dM/dlogD_p$) corresponds to the mass of particles per logarithmic size interval.

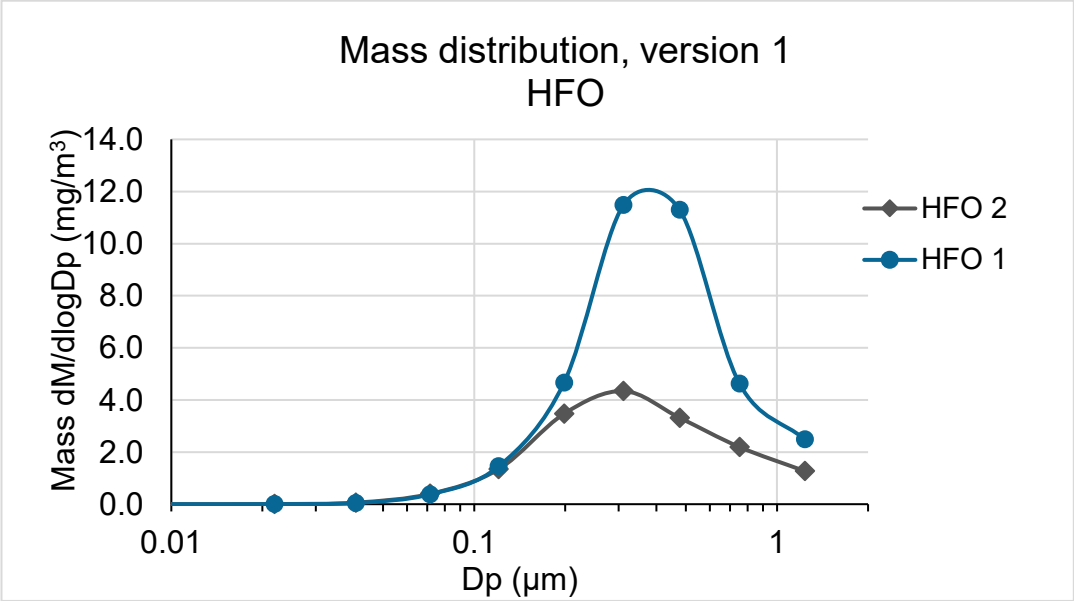

Figure 10. Mass distribution of HFO, version 1

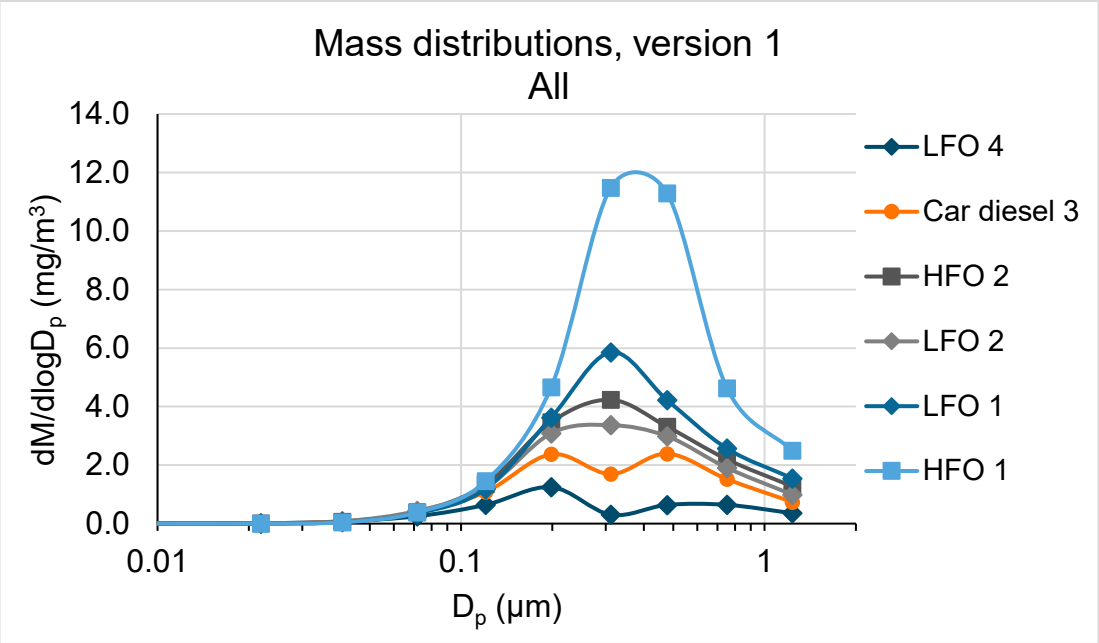

Figure 11. Particulate mass distribution for version 1 measurements. ELPI stages 1–10 are shown. The x-axis (D_p) is the aerodynamic particle diameter, and y-axis ($dM/ dlogD_p$) corresponds to the mass of particles per logarithmic size interval.

All three LFO mass distribution curves (*Figure 9*) are different in shape, especially when it comes to the oldest and newest measurements. LFO 1 is unimodal, while LFO 4 is almost bimodal. In contrast, car diesel has an even bimodal shape. The captured particle size range is the same for all LFO measurements, 0.04–1.2 µm. Both HFO measurements are similar in distribution width, and the collected particle size is similar to that of LFO (Figure 10). Studying the measurements only based on their date (*Figure 11*), the measurements change from unimodal to bimodal distribution. Graphs containing the particle number distribution ($dN/dlogD_p$) are included in the appendix, for all setup versions.

5.3.2. Version 2

Measurements in version 2 were performed in atmospheric conditions and measured directly from a small buffer tank. In *Table 6* below, PM concentrations are displayed. As before, PM is reported from ELPI stages 1–10. Because of the sudden increase in dust

concentration, ELPI records negative raw currents[9]. The raw current becomes negative when the flux of incoming and outgoing charge is unequal (Dekati Ltd., 2002). The software does not convert negative currents to mass, and thus influences the PM results drastically. The problem can be circumvented by averaging the datafile with a time interval longer than the negative reading (Dekati Ltd., 2002). However, measurements of one day were collected in the same ELPI datafile, which made it impossible to choose an averaging interval individually for all measurement peaks. Therefore, all datafiles were averaged with a 10 second period (the negative currents were estimated to last approximately 8 s). Averaging the datafiles reduced the mass and the mass distributions, but did not influence the shape of the distributions, see appendices *Figure 23*.

Table 6. PM results for version 2. Note that car diesel measurements were conducted with an injection pressure of 700 bar, while LFO and HFO measurements had the standard injection pressure of 1000 bar

Campaign #	LFO PM (1–10) [mg/m3]	Car diesel PM (1–10) [mg/m3]	HFO PM (1–10) [mg/m3]
5	1.1 ± 0.7	1.5 ± 1.1	
Averaged, 5b	0.91 ± 0.58	1.2 ± 1.1	
6	0.58 ± 0.25		2.2 ± 0.8
Averaged, 6b	0.46 ± 0.19		1.9 ± 1.0

LFO PM appears to decrease with 0.45 mg/m^3 (averaged values). Car diesel emissions are higher than those of LFO, a clear contrast to the observation in version 1. HFO particle emissions are still the highest of all measured fuels. As mentioned beforehand, the system was subject to uncontrolled dilution, and therefore the dilution ratio could not be determined. The dilution ratio influences the results significantly by making the results in *Table 6* less than the actual particle concentration in the exhaust. A more detailed explanation on the effect of dilution is found in chapter *5.4*.

[9] Raw currents are uncorrected signals from electrometers in ELPI. The data processing software contains a correction formula that redistributes small particles that are collected in the upper stages (large particles) by diffusion.

Combustion parameters are collected in Table 7. As already mentioned in version 1, a high MPI is an indication of a more complete combustion. This was true for the three fuel types. However, MPI was not sensitive enough to determine smaller changes in particle emissions, e.g. between LFO 5 and LFO 6, with the current setup. Another alternative was that the MPI was the same, but the setup caused random fluctuations in the measured particle emissions.

Table 7. CRU combustion details of version 2

Campaign #	ID [ms]	MPI [bar]
LFO 5	1.7	16
LFO 6	1.7	16
Car diesel 5	1.9	13
HFO 6	3.0	10

The same trend as with MPI was seen with ignition delay, i.e. differences in ID were only observed with fuel change. The ID followed the emitted dust level, e.g. LFO with the shortest ID had the lowest PM while HFO with longest ID had also highest PM. The effect of the lower injection pressure (car diesel) on the ID is explained in chapter *5.3.4*.

Roughly, one could say the mass distribution is bimodal, one peak in size 0.04–0.31 µm and the second in 0.31–1.2 µm, see Figure 12 and Figure 13. HFO (Figure 13) has a distinct second peak compared to LFO and car diesel. The two LFO curves (5b and 6b, Figure 12) are similar in shape and range. Figure 14 displays all the fuels together on the same scale.

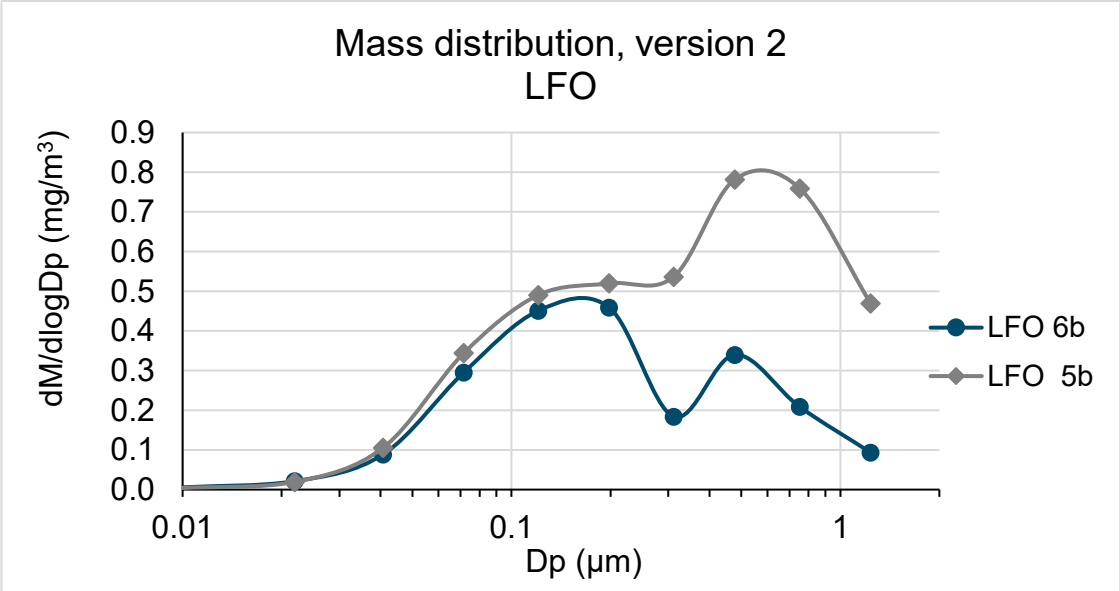

Figure 12. Mass distribution of LFO, version 2. Averaged (10 s) ELPI data was used to calculate an average distribution curve from 1–2 sets (7–14 CRU runs).

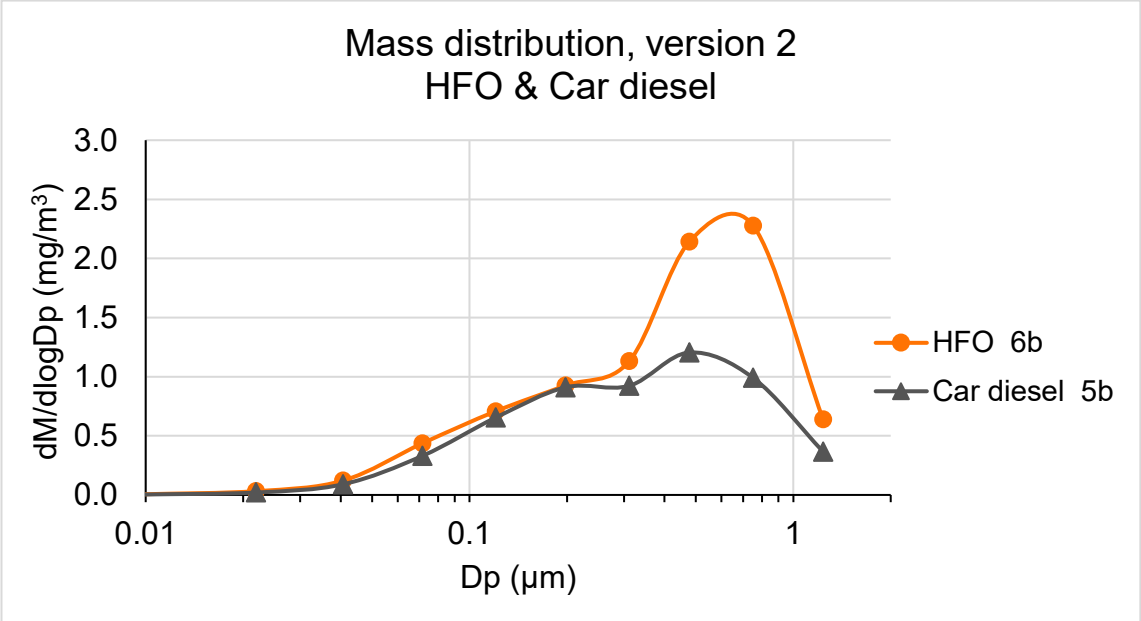

Figure 13. Mass distributions of HFO and car diesel, version 2. Averaged (10 s) ELPI data was used to calculate an average distribution curve from 1–2 sets (7–14 CRU runs).

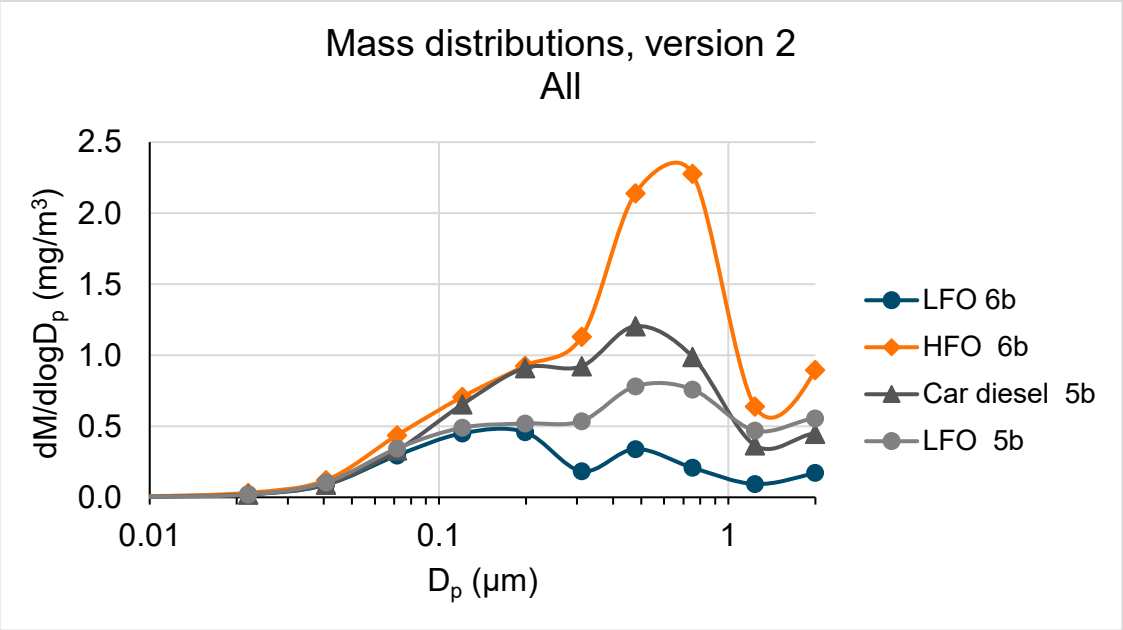

Figure 14. Particulate mass distributions of version 2 measurements. Averaged (10 s) ELPI data was used to calculate an average distribution curve from 1–2 sets (7–14 CRU runs).

5.3.3. Version 3

Setup 3 differed only slightly from version 2, with only one added valve and measurements performed at high mode. Data processing revealed that induced currents were not an issue in these measurements, hence, the unprocessed ELPI data is presented in *Table 8*. The results were three sets of seven CRU combustions each. As described previously, the first set was operated solely with valve 2, while the remaining two sets were operated with valve 2 constantly open and valve 3 (on-off) defining the introduction and closing of exhaust gases. The aim with the second method was to reduce variations in exhaust gas flow.

Table 8. LFO PM for version 3 at high mode

		Combustion data	
Set #	**LFO PM (1–10) [mg/m3]**	**MPI [bar]**	**ID [ms]**
7a	0.5 ± 0.3	12	0.87
7b	1.4 ± 0.3	12	0.87
7c	0.8 ± 0.5	12	0.86

The first impression of results in *Table 8* was that the influence of the added valve (3) remained inconclusive; the standard deviation increased marginally for 7c compared to the other two sets. Further, the mass concentration of dust increased when operating only valve 3, which might indicate that this method was more efficient in collecting particles than when controlling the measurement with valve 2.

No visible trends were seen between ignition delay and PM concentration, see *Table 8*. However, MPI repeated the trend seen in version 2 (*Table 6*), i.e. that a set with the largest pressure development also had the lowest particulate emissions. But version 3 does not have the highest MPI of all versions despite the high operation mode. In fact, LFO in version 2 at low mode had the greatest pressure-development (16 bar), while MPI of version 3 was equal to MPI of LFO in version 1 (12 bar). One possible explanation is that the injector leaked fuel during version 2 experiments. More injected fuel caused a greater pressure development.

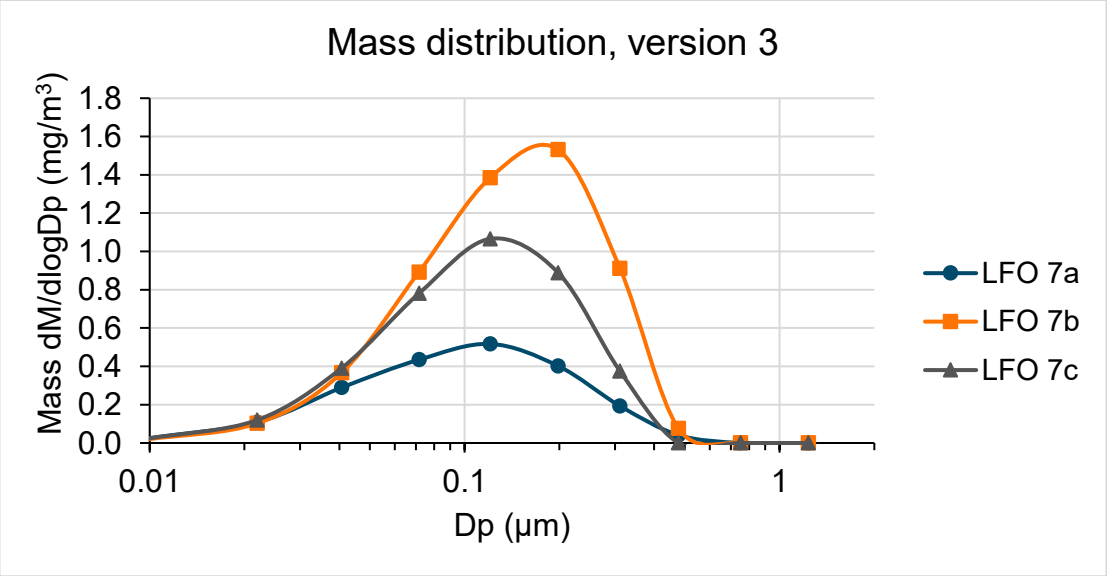

Figure 15. Particulate mass distributions of version 3 measurements.

Particulate mass distribution of set 7b is narrower and slightly more centred towards larger particles compared to set 7a and 7c (*Figure 15*). Overall, the mass distributions in version 3 are centred towards smaller particles (ca. 0.1 µm) compared to version 1 and 2 (ca. 0.2 µm respectively 0.3 µm). Additionally, version 3 distributions are unimodal, while version 2 have a skewed bimodal shape, and version 1 shows both. The shift towards smaller particles might be an indication of improved combustion at high mode.

5.3.4. Summary

Version 1 was a collection of four CRU runs, while exhaust in version 2 and 3 were measured directly of one combustion. For the sake of comparison, version 1 results were divided by 4 to obtain an approximate mass per combustion, see Table 9.

Table 9. Summary of PM results from all versions

Fuel	**Version 1 PM (1–10) [mg/m3]**		**Version 2 PM (1–10) [mg/m3]**	**Version 3 PM (1–10) [mg/m3]**
	Measured	*Per combustion*	*Per combustion*	*Per combustion*
LFO	0.9–3.9	0.22–0.97	0.46–0.91	0.5–1.4
Car diesel	3.0	0.49	1.2	
HFO	3.3–7.5	0.82–1.9	1.9	

Both LFO and HFO from version 2 align with the respective dust levels of version 1. LFO measurements (set 7a and 7c) in version 3 were in level with LFO measurements in version 2 and within the range of version 1 measurements. The only exception was set 7b, which exceeded the highest PM results in both previous versions. This was against the expectation, because a higher mode was expected to produce less dust emissions. The day after version 3 measurements the injector malfunctioned, and the high dust emissions might be due to that. If the injector leaked fuel, high PM emissions would be expected.

The PM level for car diesel is lower in the version 1 compared to version 2. The measurement in version 2 was done at an injection pressure of 700 bar while version 1 was conducted at 1000 bar. A lower injection pressure caused less fuel to be injected into the chamber and larger droplets to form. Large droplets did not oxidize as fast as small ones, and this could explain the higher PM concentration in version 2. Kuszewski et al. (2017) measured the effect of injection pressure on the ignition delay for diesel in constant-volume combustion chamber. Their observation was that a decreasing injection pressure resulted in a longer ID. This observation is confirmed in this work between version 1 and 2, where the decrease from 1000 bar to 700 bar resulted in ID extending from 1.6 ms to 1.9 ms (Table 5 and Table 7). The lower injection pressure explains the longer ID, but does not provide a theory why PM emissions are higher

despite the long ID. Here, it is reasonable to assume the measurement setups have an impact on the observed trend in PM.

5.4. Discussion

This chapter will discuss the identified shortcomings in the measurement setups and evaluate their effect on PM recorded by ELPI. First, the results are evaluated. Majority of the deficiencies are common for all versions, and these will be explored in a section about errors.

5.4.1. Evaluation of Results

The extreme reduction in LFO PM in version 1 caused majority of subsequent LFO results to fall within the range of version 1. Further, operation at high mode did not significantly reduce the mass of particles. The lower injection pressure in version 2 (car diesel) compared to version 1, aligned with the theory that increasing injection pressure reduces PM. A study with large-bore diesel engines concluded that a higher injection pressure improves soot formation, but the correlation was not strong in their results (Sarvi & Zevenhoven, 2010). Car diesel results in version 1 could not be distinguished from LFO in the same version, which was not surprising, considering their (presumed) negligible differences in composition and properties. Furthermore, a shift towards higher PM could be seen in HFO-exhaust compared to LFO in both version 1 and 2. Despite the drawbacks of the setups, the fuel composition appeared to influence the PM generated, at least between LFO and HFO. However, due to the extensive error margins (as high as 86% in version 2, car diesel) and deficient number of measurements, no definite conclusion could be drawn from these measurements.

In literature, accumulation mode particles from diesel engines are reported to range between 0.06–0.1 µm (Burtscher, 2005). It seems that the high mode of CRU shifted the mass distribution towards smaller particles compared to the low mode, see *Figure 15* respectively Figure 14. Further, mass distribution changed in version 1 from unimodal in the first measurements to bimodal in the last samples in version 1. Moreover, the bimodal behaviour continued throughout version 2 and finally changed to unimodal in the last version (3). This phenomenon was observed together with a considerable

reduction in particle mass in version 1. The varying mass distribution shape could be due to erroneous readings in ELPI, mistakes in data processing or simply random occurrences. Other potential causes are discussed below.

5.4.2. Discussion of Errors

In standardized PM measurements, such as ISO 9096 and EN13284, the number of valves and directional changes are kept to a minimum, due to the inability of large particles to follow the gas flow. Hence, the same effect occurs as in ELPI, inertial impaction, in duct corners and valves. Large particles contribute most to the mass, and thus reduced the collected weight. Especially ducts attached to the CRU were almost right angles, see for instance *Figure 8*, and are recommended to be replaced with straight ducts to minimize the loss of particles. The inertial impaction could explain the shift of the particle mass distribution towards smaller particle size between version 1 and 2. Perhaps as the duct corners collected more particles, increasingly smaller particles were captured as the duct grew narrower. In turn, the shift in particle mass distributions was observed.

Furthermore, ducts between CRU and ELPI were not trace-heated. Consequently, a temperature gradient was created between the hot gas and the cool duct wall. The difference in temperature caused particles to move towards the colder surface. This phenomenon is called thermophoresis and affects all particle sizes. The magnitude of the thermal force depends on the gas and particle properties, and on the temperature gradient (Hinds, 1982). Heating the ducts to the same temperature, or higher, as the exhaust gas eliminates the phenomenon.

In version 1 Teflon ducts were used. Teflon, or polytetrafluoroethylene, is known to accumulate negative charge, and hence is not recommended for particulate measurements. A study measuring particle losses to chamber walls in a Teflon chamber concluded that electrostatic effects dominated the removal rates of particles in sizes 0.05–1 μm (McMurry & Rader, 1985). Further, the removal rate was enhanced if particles already carried a charge. Figure 24 and Figure 25 in the appendix, present the number distributions of version 1 measurements. There, it is evident that the particle

number distribution narrows in the mentioned size range the more experiments are performed. It is likely that the electrostatic forces of the duct enhanced the effect of inertial impaction and thermophoresis in version 1.

Also in version 1, the conditions in buffer tank A, such as the long retention time (around eight minutes) and the ambient temperature, caused particle deficits and changes in particle mass distribution. After the exhaust gas had been introduced to the buffer tank, large particles immediately began to settle while small particles deposited through diffusion to tank walls. The remaining, suspended particles collided with each other and agglomerated into new particles. Reasonably, the higher the concentration, the faster the agglomeration rate. Further, for polydisperse aerosols, agglomeration was enhanced when size distribution was spread because large particles “collect” the smaller ones. Moreover, the ambient temperature of buffer tank A caused volatile components to condense onto existing particles, creating greater particles. Therefore, the residual particles in buffer tank A probably enlarged the particle size from the original. Rapid dilution to low concentration where the agglomeration rate is negligible, is the only way to “freeze” the distribution (Hinds, 1982).

As mentioned previously, the purpose with the update to version 2 was to test a plug flow concept, in which the exhaust gas would press out the air in buffer tank B. The drawbacks were identified already in the planning phase, and they were uncontrolled dilution and the location of ELPI inlet. Additional shortcomings were insufficient extraction of exhaust to ELPI, and the standardization of measurements. In version 2 and 3 the most important causes of errors were uncontrolled dilution and extraction of sample.

Uncontrolled dilution was perhaps the most significant source of error in version 2 and 3. Air was introduced to buffer tank B after the initial pressure had receded. Therefore, the exhaust was diluted with air in undefined proportions. It also entailed that the reported results were less than actual concentration. Due to the deficient proportions of mixed air, the oxygen content could be determined, which would have aided comparison of results with other studies or engine emissions.

Extraction of sample from buffer tank B was hindered by the high exhaust flow in buffer tank B. The volume flow through ELPI was 10 L/min, which was presumed to be considerably less than the flow in buffer tank B. Consequently, majority of the sample gas was wasted. A smaller sample is also less representative of the actual exhaust and suspect to random errors between individual measurements. The flow was controlled by valve 2 in version 2 and 3. Subsequently, the pressure profile of each individual measurement was controlled by this valve. Therefore repeatability was insignificant, even when the operator remained unchanged. The operator thus became a factor of error, as the efficiency of air-removal depended on the manoeuvring of the valve. In version 3, the problem was circumvented by installing an on-off valve (valve 3 in *Figure 7*). Whether the added valve brought any benefits remains inconclusive, as there were not enough data points.

5.5. Conclusion

Particle emissions were measured with three distinctive setups. Version 1 collected four CRU combustions into an 8 L tank, upon which they were measured by ELPI. The reasoning behind collecting the exhaust was to ensure sufficient amount of gases to obtain a stable reading at ELPI. This setup minimized exhaust gas losses. The container was removed for version 2 and 3, and a smaller buffer tank (ca. 0.5 L) at atmospheric pressure was used instead. The idea was to utilize a plug-flow concept, in which the high-pressure exhaust gas pressed the air from the buffer tank, upon which ELPI extracted a sample.

All setup versions were unable to produce repeatable, coherent results. Common factors of particle loss were thermophoresis and inertial impaction. The setup versions also had their individual drawbacks. Version 1 suffered from particle losses to electrostatic forces in Teflon ducts, and by settling in buffer tank A. Uncontrolled dilution and insufficient sample amount separated version 2 and 3 from version 1.

Suggestions to improve yield and repeatability were to keep valves and sharp turns to a minimum, preferably none. Further, heated duct walls, controlled and monitored dilution, and collection of entire CRU exhaust were recommended for further attempts.

In conclusion, the aim to measure the influence of fuel properties (density, sulphur and oxygen content) on PM concentration was not reached. Variations in dust mass concentration were most likely due to deficient measurement setups. This was indicated by decreasing mass concentration in version 1 and varying mass distributions. There were not enough data points to confirm with certainty that a difference in dust emissions between LFO and HFO was seen.

6. Engine Exhaust Measurement

6.1. Framework

As part of the thesis a comparison of ISO 9096 in-stack particle measurements against Electrical Low-Pressure Impactor (ELPI) was done. The measurements were performed on a testbed in Vasa during an engine's Factory Acceptance Test (FAT). A W6L32 engine was operated on LFO and 100 % load. Fuel quality was considered good, as sulphur and ash content were low (

Table 10). Another employee at Wärtsilä performed the ISO 9096 particulate measurements. The two measurements were done in parallel, and thus all engine and exhaust gas parameters were equal.

Table 10. Properties of test fuel

Property	
Density (at 15 °C, kg/m3)	835.5
Viscosity (at 80 °C, mm2/s)	1.668
Water (% V/V)	< 0.01
Ash (% m/m)	< 0.010
Sulphur (mg/kg)	13
Net Specific energy (MJ/ kg)	42.92
Calculated Cetane Index	56.7
Carbon (% m/m)	86.6
Hydrogen (% m/m)	13.8
Oxygen	<0.2

6.2. Measurement Setup

6.2.1. Total Dust Method (ISO 9096)

ISO 9096 is a standardized filter method for PM validation. In short, exhaust gas is passed through a pre-weighed and dried filter either inside or outside the stack. In-stack measurements were done for the project. Measurements are done isokinetically, which

essentially means the flow rate through the filter is the equal to that of the exhaust gas. Afterwards, the filter is dried and weighed to measure the mass of collected particles. Finally, the dust mass concentration in engine exhaust can be calculated from the acquired mass and flow rate.

6.2.2. ELPI Measurement

For comparative purposes ELPI was used. See chapter *5.1.2* for the operation principle of ELPI. As before, impactor stages 1–10 (0.01–1.2 µm) were utilized for determining PM concentration from current. Due to temperature constraint of 60 °C by ELPI the exhaust sample was first diluted with hot, dry air (175 °C) and then with cool, dry air (ambient temperature). For both dilutions the dilution ratio (DR) is 8, i.e. final DR was 64. The measurement setup can be seen in *Figure 17* and *Figure 16*.

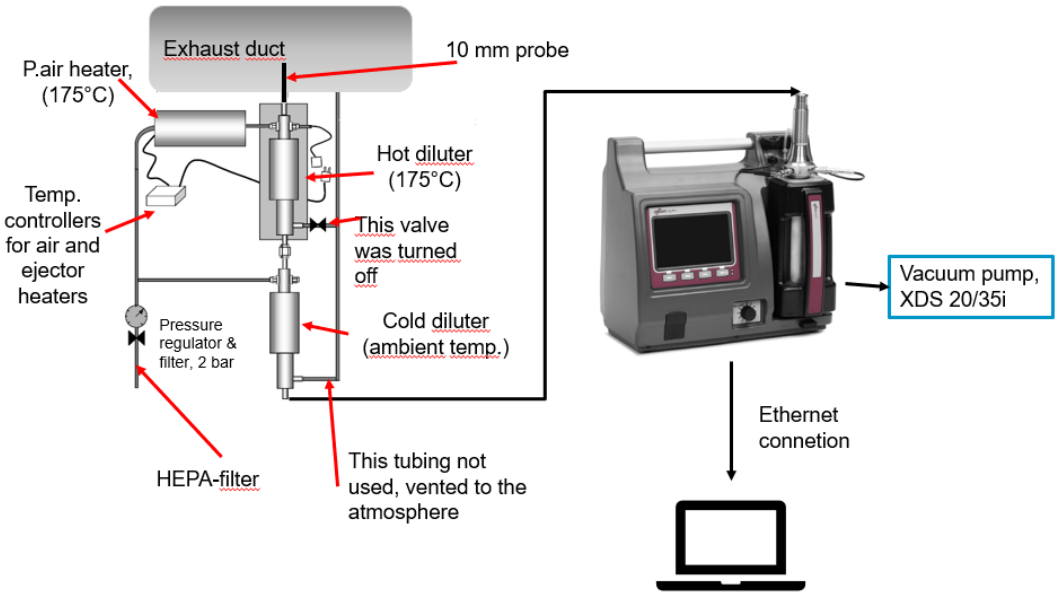

Figure 16. Schematic view of ELPI measurement setup (double dilution setup by Dekati®).

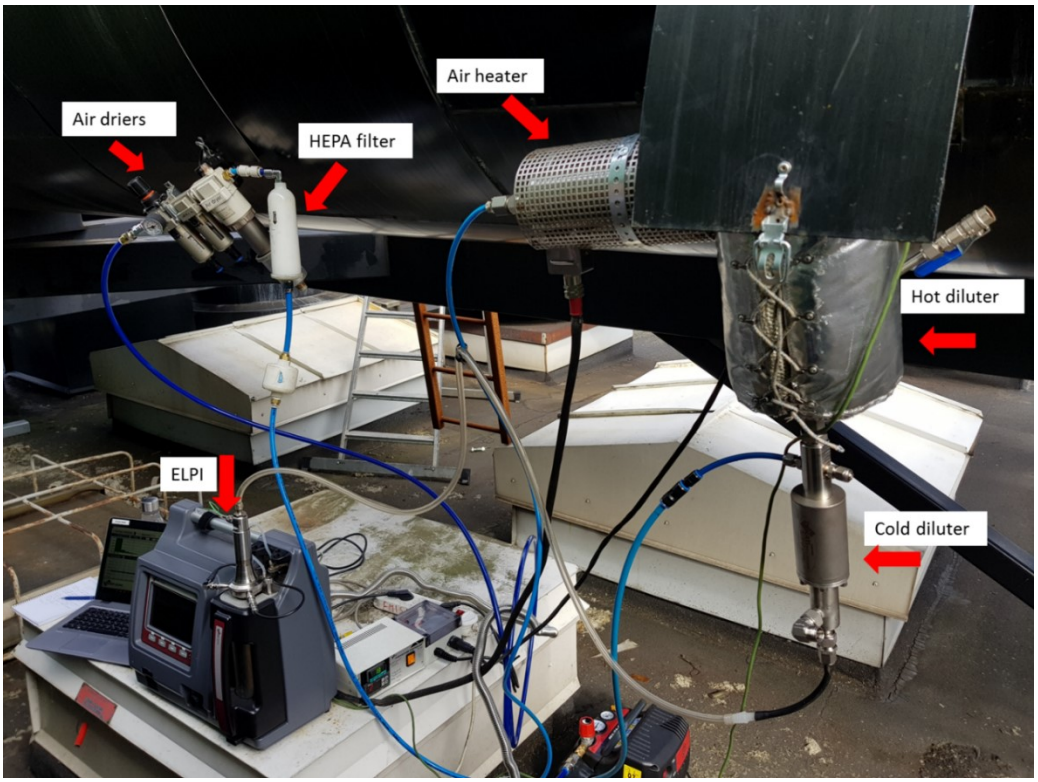

Figure 17. ELPI measurement setup.

6.3. Results

ISO 9096 PM result is an average of three samples, all of which lasted 28 minutes. The results are seen in Table 11. The result fulfils the BAT limit of 10 mg/Nm^3 (dry, 15 vol-% O_2).

Table 11. ISO 9096 in-stack results, converted to dry mg/Nm3 at 15 vol-% oxygen. Total PM is the average of the three samples

Sample #	**ISO 9096 PM result**
	mg/ Nm^3 (dry, 15 vol-% O_2)
1	8.69
2	8.51
3	8.01
PM, average	8.40

Similar intervals (28 min) as that of the ISO measurement were used to determine ELPI PM concentration. ELPI reports dust concentration as mg/m^3 (*Table 12*), which was

converted to mg/Nm^3 (dry, 15 vol-% O_2). Exhaust gas parameters and the volume flow in the stack are equal for both measurements (ISO and ELPI). The calculation of the ELPI results is in the appendices of this document.

Of the 14 stages in ELPI, only 1–10, i.e. particle sizes 0.01–1.2 µm, were used for mass determination. Diesel particles are commonly assumed to be accumulation mode particles, i.e. 60–100 nm in size (Burtscher, 2005). As previously mentioned, distillate fuel particles are considered <1.2 µm in diameter, and hence larger particle sizes (stages 11–14, i.e. 2–7.3 µm) are excluded. The DR is already considered in the unconverted data in *Table 12*.

Table 12. Raw and converted ELPI PM emissions, stages 1–10

Sample #	**PM, original**	**PM, normalized**
	mg/m^3	*mg/Nm^3 @ 15 vol-% O_2, dry*
1	2.10	3.40
2	2.78	4.53
3	3.07	5.06
Average		**4.33**

6.4. Discussion

The first observation was that ISO 9096 PM concentration was approximately double the PM concentration recorded by ELPI. The total dust method was subjected to coarse mode particles, i.e. particles released from duct walls. These particles were not carried into the ELPI probe. Also, the different measuring temperatures of ISO 9096 and the ELPI setup were likely to influence the recorded mass. Particles were collected on the filter in temperatures around 300 °C, while ELPI recorded particles in ambient temperature. If solely the influence of temperature was studied, the ambient temperature in ELPI would enhance condensation, which would result in higher PM concentration for ELPI than for the total dust method, which contradicts the observed results. But, as ELPI was preceded by double dilution, the dilution parameters affected the recorded mass. High DR led to decreased PM, because vapour phase concentration decreased. As vapour phase concentration was reduced, nucleation of these components declined until a

critical DR was reached when no or negligible nucleation of semi-volatile compounds occurred (Ushakov, Valland, Nielsen, & Hennie, 2014). In other words, a too high DR prevented nucleation of volatile components. Therefore, less mass was recorded because volatiles passed ELPI.

A requirement in the total dust method was isokinetic conditions at probe, which entailed two criteria to be met: 1) the gas flow velocity was the same in both the probe-inlet and the stack 2) the probe was aligned in the direction of the gas flow (Hinds, 1982). The second criterion was not fulfilled, as the ELPI probe was perpendicular to the exhaust gas flow. Consequently, large particles were not entrained by the probe, which resulted in less recorded mass (Hinds, 1982). However, these could also be discarded in the chosen ELPI-range. Further, whether the volume flow in the probe equalled that of the surrounding gas can be considered negligible (Burtscher & Majewski, 2016).

ELPI is not accurate when it comes to determining mass concentration. According to Maricq et al. (2006) ELPI overestimates PM. However, this was already considered when stages 11–14 are excluded from the calculation. Further, the authors conclude that ELPI has a 20 % uncertainty when determining PM. The ISO method is not either without uncertainty. A study by VTT compared PM determination (EN 13284-1) of nine laboratories (Kajolinna et al., 2014). The laboratories reported their measurement uncertainties of LFO PM concentration, and the uncertainties varied from ±9 % to ±121 %. Another study generated a controlled mixture of soot and hydrocarbon vapour (pentadecane) to determine the artefact on Teflon-coated glass fibre filters. At low particle concentration (0.13 mg/m^3), the positive artefact was 31 % of the collected soot (Högström et al., 2012). However, their concentration was significantly lower than the PM concentration obtained in this work and thus not transferrable to the current results. For further studies of the gravimetric artefact, it is recommended to verify the amount of adsorbed hydrocarbons with two filter in series, as in the study by Högström et al. (2012).

The second observation was that ELPI dust mass concentration increased with time, while the opposite was true for the total dust measurement. ELPI mass concentration distribution (*Figure 18*) indicated an increase in particles greater than 0.20 µm from

sample 1 to 3. The rising exhaust gas temperature could be connected to this observation. Temperature of samples 1–3 increased in the following order: 311 °C, 315 °C, 322 °C. Higher temperature in the stack could cause less volatile hydrocarbons to be attached to the filter in ISO-method, and thus explaining the phenomenon. The percental increase in temperature was below or equal to 2 %. The decrease in mass concentration was 2 % (sample 1 to 2) and 6 % (sample 2 to 3). Considering the low percental, the results cannot be said to correlate.

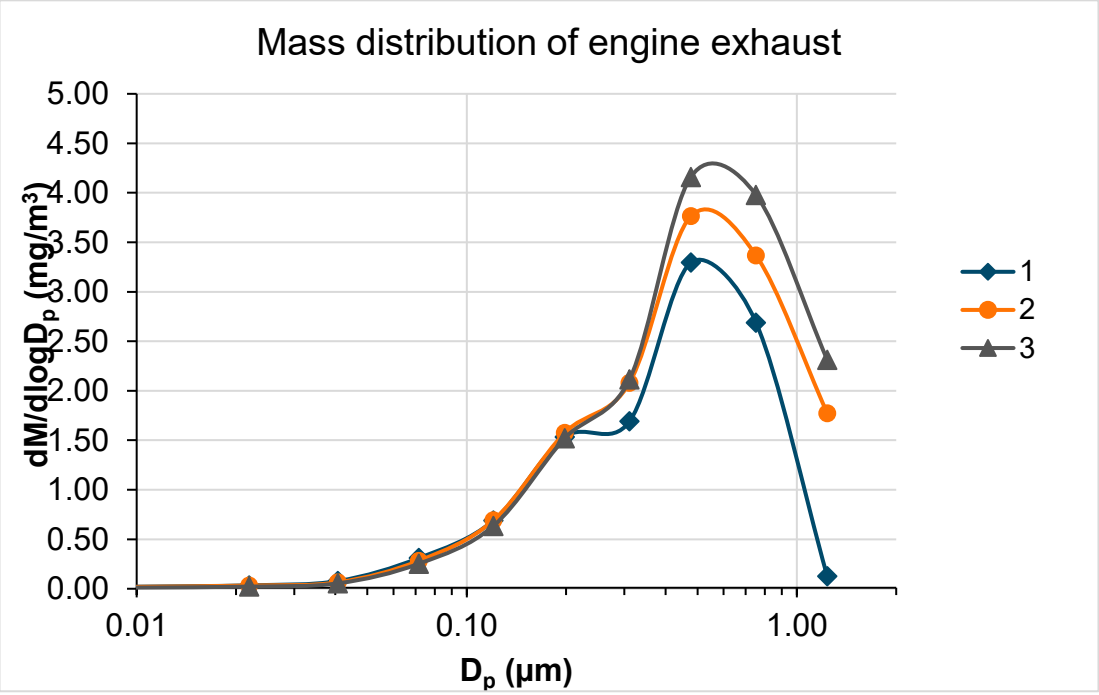

Figure 18. Mass distribution of samples 1–3 with ELPI (stage 1–10) for W6L32 exhaust. Corresponding figure with number distribution can be found in the appendices.

6.5. Conclusion

In engine exhaust ELPI measured approximately half the mass concentration of the ISO 9096 method, 4.33 respectively 8.40 mg/Nm^3 (dry, 15 vol-% O_2). The result was surprising, as the ELPI was expected to record a higher PM concentration. One considered aspect was that the methods are completely different: ISO 9096 measures mass, while ELPI measures current. Discrepancies could have occurred from the measurement uncertainties of both ELPI and the ISO method. Also the effect of dilution ratio and temperature in ELPI setup influenced whether volatiles condensed onto particles. Additionally, gaseous hydrocarbons could have adsorbed on the filter in the gravimetric method. Furthermore, the setups were dissimilar: the total dust method collected the sample directly inside the duct, while the sample measured by ELPI was diluted 64 times in two different temperatures. Hence, a direct comparison was unfeasible to make.

For a comparison to be feasible, all the measurement methods should be as equal as possible. Comparison of ELPI and filter methods could be realized by changing ISO 9096 to ISO8178[10], and would thus align the current ELPI setup with a gravimetric method. Alternatively, engine ELPI measurements could be performed with only hot dilution to align it with in-stack conditions. Elevated temperature dilution would ensure closer resemblance to ISO 9096.

[10] ISO8178-1 Reciprocating internal combustion engines- Exhaust emission measurement is a standard for non-automotive diesel engines that developed for both gaseous and particulate emissions.

7. Comparison of Engine and CRU Emissions

This chapter attempts to evaluate the difference between the acquired particle emissions from the CRU and the engine. The purpose of the comparison is to estimate the difference in particulate emissions between the pilot-scale and the engine. The shortcomings of both campaigns are already discussed in previous chapters. CRU measurements from version 1 are included. As the system is closed in version 1, it is assumed to have the highest yield of particulate emissions and bears the closest resemblance to the ISO method compared to the open-system versions.

Both engine and the selected CRU measurements were operated with LFO. As can be seen in Table 13, the fuel properties were similar in most aspects. The most prominent differences were density and viscosity, which suggested the distillation range was lower for the LFO used in engine measurements, i.e. it contained less high-molecular weight chains than the CRU fuel. Sulphur content was higher in the engine fuel. Nevertheless, the fuel properties are excluded from the comparison. Any influence of a specific fuel property on particulate emissions is most likely overshadowed by the mechanical and physical differences of the systems.

Table 13. Comparison of LFO fuel properties in engine and CRU measurements

Property	**Unit**	**Engine**	**CRU**
Density	at 15 °C, kg/m3	835.5	840.7
Viscosity	at 80 °C, mm2/s	1.668	1.808
Ash	% m/m	< 0.010	< 0.010
Sulphur	mg/kg	13	<10
Net Specific energy	MJ/ kg	42.92	42.84
Calculated Cetane Index		56.7	56
Carbon	% m/m	86.6	86.9
Hydrogen	% m/m	13.8	13.7

7.1. Results

To enable adequate comparison, results from both the CRU and the engine were converted to the same unit, i.e. mass per energy input of fuel (mg/MJ). Upon changing the unit from particle mass per exhaust gas volume (mg/m^3) to particle mass per fuel input (mg/MJ), uncertainties in the CRU exhaust gas conditions were discarded. Naturally the new unit was not without shortcomings, but due to the above-mentioned reason it was perceived more reliable for the comparison.

The recalculated CRU results presented in *Table 14* assumed 100 % fuel conversion efficiency. The fuel consumption of CRU was unknown in these experiments. However, a previous experiment[11] at low temperature (40–50 °C) deduced the approximate energy injected. The lower heating value (LHV) of the test-LFO was 42.7 MJ/kg, which was close to the fuel in CRU experiments in this work (*Table 13*). The previous experiment concluded that 2207 J per injection was introduced, and this was value was applied when converting the current CRU results. Also the four CRU combustions were accounted for.

Table 14. Particulate mass per input fuel energy (mg/MJ). Converted LFO measurements from CRU version 1 (low mode) are presented. All ELPI results are from stages 1–10 (particle diameter 0.01–1.2 µm)

	Engine		**CRU**
Sample #	ELPI	ISO 9096	ELPI version 1.
	mg/MJ	*mg/MJ*	*mg/MJ*
1	2.5	6.4	15
2	3.4	6.5	11
3	3.8	6.0	3.3
Average	3.2	6.3	9.7

[11] Mass of fuel from 10 injections was measured at an injection pressure 1000 bar, and injection period of 1000 µs. When the energy content (as LHV) of the fuel is known, energy per injection was deduced.

The conversion of engine PM concentration to mass per energy content of fuel was approximated from the specific fuel consumption. This approximation was decided to be sufficiently close for the comparison at hand. Calculations for both engine and CRU results are found in the appendices.

As illustrated in Table 14, both ELPI and ISO 9096 determine particle emissions from the W6L32 engine to be lower than from the CRU. The result was expected, and the following two reasons were considered the most prominent. First, the in-cylinder conditions (temperature and pressure) are substantially higher in the engine cylinder than in the static chamber. Second, less mixing of reactant occurs in the CRU. In an engine the moving piston increases fuel-air mixing and thus more reactions reach completion. As was previously observed in chapter *5.3.1*, the particle level decreases steadily in version 1. Sample 3 from the CRU is in the range of ELPI recordings from the engine. In the current comparison, the engine particle emissions by ELPI and ISO 9096 are 67 % respectively 35 % less than CRU particle emissions.

7.2. Discussion

The discussion below will focus on the CRU because the combustion chamber is the primary equipment in this work and is more available for modifications.

One identified shortcoming in converting the CRU results from PM concentration to PM per energy of fuel, was that the actual temperature of the fuel injected was unknown. As the injector heated up, fuel viscosity was reduced, and thus more fuel was injected than currently accounted for. The CRU would thus emit less particles per fuel input, and the difference to the engine emissions would grow narrower. A study measured that the viscosity of LFO decreased 40 % when fuel temperature increased from 50 °C to 75 °C, and 60 % with a temperature increase from 50 °C to 100 °C (Schaschke, Fletcher, & Glen, 2013). Knowledge about the CRU fuel consumption is necessary for further studies. Hu et al. (2013) calibrated their CRU by performing >100 injections with defined operational parameters in ambient conditions. Since no combustion occurred, the mass of fuel collected in the chamber was measured. This method is time-consuming as it involves

removing the chamber, but it could be an option when the same operational parameters are used for extensive measurement campaigns.

The injector test, which the fuel amount was based on, was done in atmospheric pressure. As the pressure in the chamber was considerably higher than in the injector test, the pressure against the nozzle orifices caused less fuel to be injected. Consequently, the current CRU result would be greater in value and the difference to engine emissions larger.

Other reasons that influence the mass of fuel injected in CRU are the injector wear and deposit build-up on the nozzle. These could impact the injected fuel amount randomly. Outside the experiments of this work, the CRU was operated on fuels ranging from crude oil to LFO. Thus, the nozzle was prone to wear and accumulation of deposits. Thus, it is recommended to choose an injector suitable for the fuel of study, or to change the injector with regular intervals.

7.3. Conclusion

To enable comparison between CRU and engine results, PM concentration was converted to mass per energy injected (mg/MJ). The engine particle emissions by ELPI and ISO 9096 were 67 % respectively 35 % less than CRU particle emissions. The discrepancy was concluded to originate from the in-cylinder conditions (higher temperature and pressure) in the engine and due to the poorer fuel-air mixing in the static combustion chamber. For further research it was suggested to calibrate the CRU fuel injection and to maintain the injector regularly.

8. Conclusion

The stricter limit on PM in the published LCP BAT challenges power plants to consider particulate emissions in their design. The PM limit of 10 mg/Nm^3 (at 15 vol-% oxygen and standard conditions) is currently only possible to reach (without exhaust gas cleaning) with high-quality LFO on Wärtsilä's diesel engines. The aim of this study was to determine how selected fuel properties influence the particle mass concentration in a constant-volume combustion chamber, a Combustion Research Unit (CRU) manufactured by Fueltech. The aim of this work is of interest because studies measuring quantitatively particulate mass from a constant-volume chamber of diesel fuel are limited.

Based on the literature study, three fuel properties were chosen to be studied in the experimental section. Aspects under focus in this work were density, sulphur content and oxygen content. A high density indicates of heavy molecules present from the back-end of the distillation curve. Thus more PM were expected with high density. Due to sulphur's strong influence on PM it was motivated to investigate the impact of sulphur content in fuel on particulate. As with density, a high sulphur content was predicted to result in more PM. The third fuel parameter of interest was the oxygen content. The primary target of oxygenates (oxygen-containing additives) is soot, which led to the hypothesis that PM decreases with an increase in oxygen amount in the fuel.

Particle mass concentrations were measured with three distinctive setups. All setup versions were unable to produce repeatable, coherent results. This was evident when no difference in PM concentration could be distinguished between LFO and HFO due to the high uncertainty. Common factors of particle loss were most likely thermophoresis and inertial impaction. Other particle phenomena suspected to influence PM concentration were settling, electrostatic forces, uncontrolled dilution and insufficient sample amount. The aim to measure the influence of fuel properties on PM concentration was not reached.

The opportunity to perform fuel tests in small scale is valuable for understanding fuel combustion behaviour and particle emissions. Suggestions for future research were to

keep valves and sharp duct bends to a minimum, preferably none. Further, heated duct walls, controlled and monitored dilution, and collection of entire CRU exhaust were recommended.

A Wärtsilä W6L32 engine was operated on LFO and 100 % load. Both an in-stack total dust method (ISO 9096) and an Electrical Low-Pressure Impactor (ELPI) with double-dilution were used to measure PM concentration. ELPI is designed to determine particle number but can be used to approximate particle mass. In these engine conditions and with this measurement setup, ELPI measured approximately half the mass concentration of the total dust method, 4.33 respectively 8.40 mg/Nm^3 (dry, 15 vol-% O_2). The discrepancies were concluded to originate from the fundamental difference in how particles were measured and from the dilution conditions.

The purpose of determining the PM concentration in engine exhaust was to deduce an indicative value of the difference in dust concentration between the CRU and an engine. The PM concentration was converted to mass per energy injected (mg/MJ). The engine particle emissions by ELPI and ISO 9096 were 67 % respectively 35 % less than CRU particle emissions. The discrepancy was concluded to originate from the in-cylinder conditions (higher temperature and pressure) in the engine and due to the poorer fuel-air mixing in the static combustion chamber. Further improvement suggestions for the CRU were to calibrate the fuel injection and to maintain the injector regularly.

Bibliography

Aakko-Saksa, P., Koponen, P., Aurela, M., Vesala, H., Piimäkorpi, P., Murtonen, T., . . . Kuittinen, N. (2018). Considerations in analysing elemental carbon from marine engine exhaust using residual, distillate and biofuels. *Journal of Aerosol Science*, *126*, 191-204.

Aakko-Saksa, P., Vesala, H., Koponen, P., Nyyssönen, S., Puustinen, H., Lehtoranta, K., . . . Karjalainen, P. (2016). Black carbon measurements using different marine fuels. In *28th CIMAC World Congress.*

Anderson, M., Salo, K., Hallquist, Å M., & Fridell, E. (2015). Characterization of particles from a marine engine operating at low loads. *Atmospheric Environment*, *101*, 65-71.

Andreae, M. O., & Gelencsér, A. (2006). Black carbon or brown carbon? the nature of light-absorbing carbonaceous aerosols. *Atmospheric Chemistry and Physics, 6*(10), 3131-3148.

Betts, W. E., Fløysand, S. Å, & Kvinge, F. (1992). *The influence of diesel fuel properties on particulate emissions in European cars*. (No. 922190).SAE Technical Paper.

Bonczyk, P. A. (1991). Effect of ferrocene on soot in a prevaporized iso-octane/air diffusion flame. *Combustion and Flame, 87*(3-4), 233-244.

Burtscher, H. (2005). Physical characterization of particulate emissions from diesel engines: A review. *Journal of Aerosol Science, 36*(7), 896-932.

Burtscher, H., & Majewski, W. A. (2016). Exhaust gas sampling and conditioning. Retrieved from https://www.dieselnet.com/tech/measure_sample.php

Cowley, L. T., Stradling, R. J., & Doyon, J. (1993). *The influence of composition and properties of diesel fuel on particulate emissions from heavy-duty engines*. (No. 932732).SAE Technical Paper.

Dekati Ltd. (2002). *Negative current values in ELPI+ data*

Dekati Ltd. (2016). *Dekati ELPI+ USER MANUAL* (1.54th ed.)

Eastwood, P. (2008). *Particulate emissions from vehicles*. Chichester [u.a.]: Wiley.

EN13284-1:2017. (2017). *Stationary source emissions - determination of low range mass concentration of dust - part 1: Manual gravimetric method*. (). Brussels, Belgium: European Committee for Standardization.

European Parliament & Council of the European Union. (2016). *Regulation (EU) 2016/1628 of the European Parliament and of the Council of 14 September 2016 on requirements relating to gaseous and particulate pollutant emission limits and type-approval for internal combustion engines for non-road mobile machinery*. Luxembourg: Office for Official Publications of the European Communities.

Ghojel, J. I., & Tran, X. (2010). Ignition characteristics of diesel− water emulsion sprays in a constant-volume vessel: Effect of injection pressure and water content. *Energy & Fuels, 24*(7), 3860-3866.

Giechaskiel, B., Maricq, M., Ntziachristos, L., Dardiotis, C., Wang, X., Axmann, H., . . . Schindler, W. (2014). Review of motor vehicle particulate emissions sampling and measurement: From smoke and filter mass to particle number. *Journal of Aerosol Science, 67*, 48-86.

Glassman, I., & Yetter, R. A. (2008). *Combustion* (4. ed.). Amsterdam [u.a.]: Elsevier.

Heywood, J. B. (1988). *Internal combustion engine fundamentals*. New York u.a: McGraw-Hill.

Hinds, W. C. (1982). *Aerosol technology*. New York [u.a.]: Wiley.

Högström, R., Karjalainen, P., Yli-Ojanperä, J., Rostedt, A., Heinonen, M., Mäkelä, J. M., & Keskinen, J. (2012). Study of the PM gas-phase filter artifact using a setup for mixing diesel-like soot and hydrocarbons. *Aerosol Science and Technology, 46*(9), 1045-1052.

Hu, Z., Somers, L., Davies, T., McDougall, A., & Cracknell, R. F. (2013). A study of liquid fuel injection and combustion in a constant volume vessel at diesel engine conditions. *Fuel, 107*, 63-73.

ISO 9096:2017 (E). (2017). *Stationary source emissions- manual determination of mass concentration of particulate matter*. (). Geneva, Switzerland: International Organization for Standardization.

Jääskeläinen, H., & Khair, M. K. (2015). Common rail fuel injection. Retrieved from https://www.dieselnet.com/tech/diesel_fi_common-rail.php#large

Jääskeläinen, H., & Khair, M. K. (2017). Combustion in diesel engines. Retrieved from https://www.dieselnet.com/tech/diesel_combustion.php#heat

Kalghatgi, G. T. (2014). *Fuel/engine interactions* SAE International.

Karila, K., Kärkkäinen, T., Larmi, M., Niemi, S., Sandström, C. E., Tamminen, J., & Tiainen, J. (2004). Reduction of particulate emissions in compression ignition engines. *Otamedia, Espoo, Finland.*

Kittelson, D. B. (1998). Engines and nanoparticles: A review. *Journal of Aerosol Science, 29*(5), 575-588.

Kook, S., & Pickett, L. M. (2011). Soot volume fraction and morphology of conventional and surrogate jet fuel sprays at 1000-K and 6.7-MPa ambient conditions. *Proceedings of the Combustion Institute, 33*(2), 2911-2918.

Kupareva, A., Mäki-Arvela, P., Grénman, H., Eränen, K., Sjöholm, R., Reunanen, M., & Murzin, D. Y. (2012). Chemical characterization of lube oils. *Energy & Fuels, 27*(1), 27-34.

Kuszewski, H., Jaworski, A., Ustrzycki, A., Lejda, K., Balawender, K., & Woś, P. (2017). Use of the constant volume combustion chamber to examine the properties of autoignition and derived cetane number of mixtures of diesel fuel and ethanol. *Fuel, 200*, 564-575.

Lapuerta, M., Hernández, J. J., Fernández-Rodríguez, D., & Cova-Bonillo, A. (2017). Autoignition of blends of n-butanol and ethanol with diesel or biodiesel fuels in a constant-volume combustion chamber. *Energy, 118*, 613-621.

Lecomte, T., Ferrería de la Fuente, José Félix, Neuwahl, F., Canova, M., Pinasseau, A., Jankov, I., . . . Delgado Sancho, L. (2017). *Best available techniques (BAT) reference document for large combustion plants*. (). Luxembourg, Publications Office of the European Union: European Commission, Joint Research Centre.

Lee, K. O., Zhu, J., Ciatti, S., Yozgatligil, A., & Choi, M. Y. (2003). *Sizes, graphitic structures and fractal geometry of light-duty diesel engine particulates*. (No. 2003-01-3169).SAE Technical Paper.

Liang, Z., Chen, L., Alam, M. S., Rezaei, S. Z., Stark, C., Xu, H., & Harrison, R. M. (2018). Comprehensive chemical characterization of lubricating oils used in modern vehicular engines utilizing GC× GC-TOFMS. *Fuel, 220*, 792-799.

Lyyränen, J., Jokiniemi, J., Kauppinen, E. I., & Joutsensaari, J. (1999). Aerosol characterisation in medium-speed diesel engines operating with heavy fuel oils. *Journal of Aerosol Science, 30*(6), 771-784.

Maricq, M. M., Xu, N., & Chase, R. E. (2006). Measuring particulate mass emissions with the electrical low pressure impactor. *Aerosol Science and Technology, 40*(1), 68-79.

McMurry, P. H., & Rader, D. J. (1985). Aerosol wall losses in electrically charged chambers. *Aerosol Science and Technology, 4*(3), 249-268.

Miller, A. L., Stipe, C. B., Habjan, M. C., & Ahlstrand, G. G. (2007). Role of lubrication oil in particulate emissions from a hydrogen-powered internal combustion engine. *Environmental Science & Technology, 41*(19), 6828-6835.

Moulijn, J. A., Makkee, M., & van Diepen, A. E. (2013). *Chemical process technology* (2nd ed.). Chicester: Wiley.

Oberdörster, G., Sharp, Z., Atudorei, V., Elder, A., Gelein, R., Kreyling, W., & Cox, C. (2004). Translocation of inhaled ultrafine particles to the brain. *Inhalation Toxicology, 16*(6-7), 437-445.

Rabl, S., Davies, T. J., McDougall, A. P., & Cracknell, R. F. (2015). Understanding the relationship between ignition delay and burn duration in a constant volume vessel at diesel engine conditions. *Proceedings of the Combustion Institute, 35*(3), 2967-2974.

Sarvi, A., & Zevenhoven, R. (2010). Large-scale diesel engine emission control parameters. *Energy, 35*(2), 1139-1145.

Sarvi, A., Fogelholm, C., & Zevenhoven, R. (2008). Emissions from large-scale medium-speed diesel engines: 2. influence of fuel type and operating mode. *Fuel Processing Technology, 89*(5), 520-527.

Sarvi, A., Lyyränen, J., Jokiniemi, J., & Zevenhoven, R. (2011). Particulate emissions from large-scale medium-speed diesel engines: 2. chemical composition. *Fuel Processing Technology, 92*(10), 2116-2122.

Schaschke, C., Fletcher, I., & Glen, N. (2013). Density and viscosity measurement of diesel fuels at combined high pressure and elevated temperature. *Processes, 1*(2), 30-48.

Tornehed, P. (2010). *Particulate emissions associated with diesel engine oil consumption*. (PhD dissertation). KTH, Stockholm. Retrieved from http://urn.kb.se/resolve?urn=urn:nbn:se:kth:diva-25880

Ushakov, S., Valland, H., Nielsen, J. B., & Hennie, E. (2013). Particle size distributions from heavy-duty diesel engine operated on low-sulfur marine fuel. *Fuel Processing Technology, 106*, 350-358.

Ushakov, S., Valland, H., Nielsen, J. B., & Hennie, E. (2014). Effects of dilution conditions on diesel particle size distribution and filter mass measurements in case of marine fuels. *Fuel Processing Technology, 118*, 244-253.

Wang, L., Song, C., Song, J., Lv, G., Pang, H., & Zhang, W. (2013). Aliphatic C–H and oxygenated surface functional groups of diesel in-cylinder soot: Characterizations and impact on soot oxidation behavior. *Proceedings of the Combustion Institute, 34*(2), 3099-3106.

Warnatz, J., Dibble, R. W., & Maas, U. (2006). *Combustion* (4th ed.). Berlin; Heidelberg; New York: Springer.

Westerholm, R., & Egebäck, K. (1994). Exhaust emissions from light-and heavy-duty vehicles: Chemical composition, impact of exhaust after treatment, and fuel parameters. *Environmental Health Perspectives, 102*(suppl 4), 13-23.

Wright, A. A. (2000). *Exhaust emissions from combustion machinery*. London: Institute of Marine Engineers.

Appendices

1. CRU measurement

1.1. Details of system components

- Connection between CRU and buffer tank were stainless steel pipe, not trace heated. Diameter (inner): 4 mm
- Ducts between buffer tank A and B and buffer tank B and ELPI were Teflon (version 1). Not trace heated. Diameter (inner): 6.94 mm
- Buffer tank A, unknown material, volume**:** 8 L
- Buffer tank B, stainless steel, volume**:** 0.5 L
- Copper pipe: Premium 6.00*0.80 EN1057. Diameter (inner): 4 mm

Layouts of buffer tank A and B, version 1

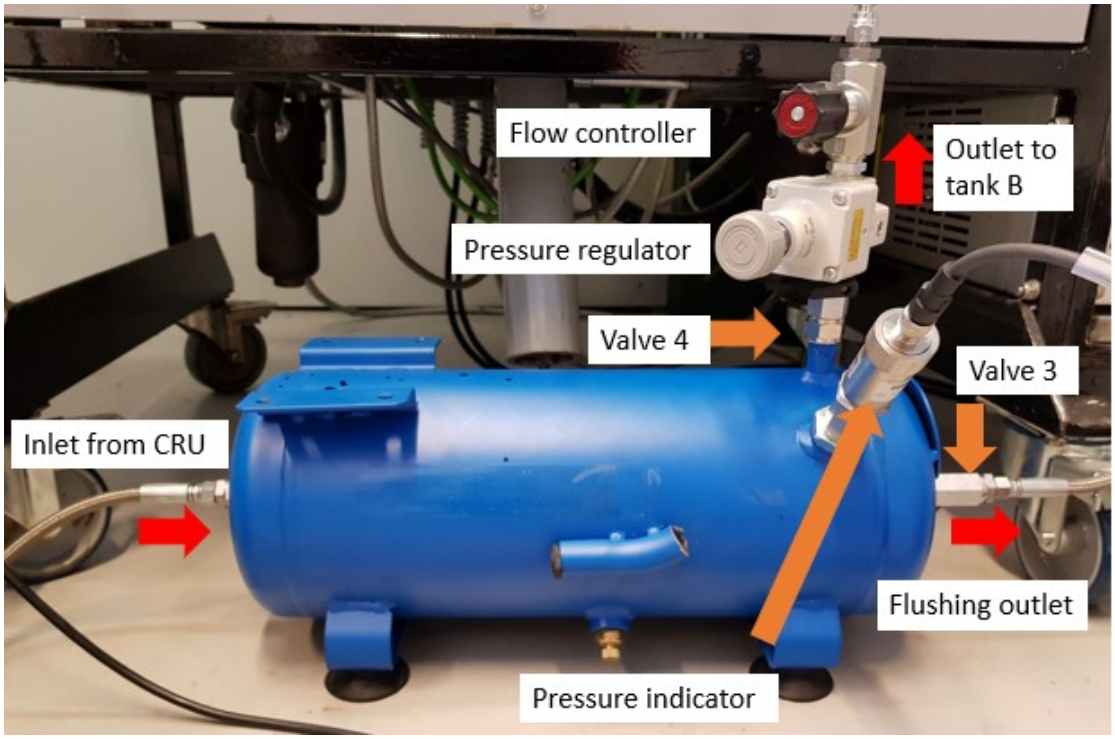

Figure 19. View of connections for buffer tank A. Red arrows indicate flow direction, while orange arrows refer to components.

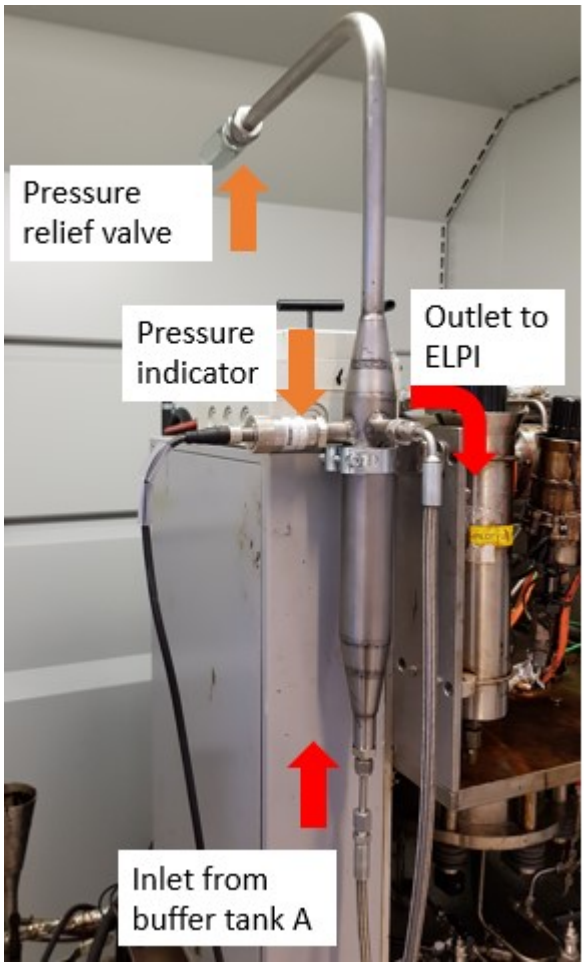

Figure 20. Connections for buffer tank B in version 1. Red arrows are flow direction, while orange arrows refer to components.

1.2. Dust deposits in buffer tank A, version 1

The interior of buffer tank A was checked with an endoscope. The interior surface looked uneven and had random dark spots (like oil splashes). In addition, upon unscrewing parts from buffer tank A, the inlet from CRU had collected a deposit of brown dust, see *Figure 21*. When inspecting with a microscope, the deposit was found to consist of both black and brown particles, see *Figure 22*. The dust is a collection from all three fuels, most likely consisting of soot and ash particles. No further analyses were performed.

Figure 21. Dust deposit on buffer tank A inlet from CRU.

Figure 22. Microscope picture of dust from buffer tank A.

1.3. Data processing

1.3.1. Version 1

2. Collected 4 CRU runs into buffer tank A ➔ 1 ELPI measurement
3. 4–14 ELPI measurements were made per fuel in day, depending on the time available. (12–56 CR runs)
4. Measurement peaks are selected in the ELPI software by selecting the time interval with an accuracy of 1 s.
5. The software converts current/s to mg/m^3 in the selected time interval, for all 14 impactor stages in ELPI.
6. Only stages 1–10 are accounted for in mass.
7. The calculated mass results for the day's ELPI recordings (measurements) averaged, and these are the results found in Table 4.
8. CRU parameters reported in the document are averages unless stated otherwise. Which combustions that are measured in ELPI cannot be determined, and thus the reported parameter values are averages of all CRU runs, even those that were not measured in ELPI (during an ELPI measurement, CRU ran in its normal mode).

1.3.2. Version 2

2. One CRU shot was directly measured by ELPI.
3. The standard CRU combustion series consist of 7 runs, and thus 7–14 ELPI measurements are made per fuel. Measurements that for some evident reason are not representative have been removed, e.g. if a valve was closed too late, air was introduced to the buffer tank, which influenced the ELPI reading.
4. The datafile of the day was averaged with 10 s.
5. Measurement peaks are selected in the ELPI software by selecting the time interval with an accuracy of 1 s.
6. The software converts current/s to mg/m^3 in the selected time interval, for all 14 impactor stages in ELPI.
7. Only stages 1–10 are accounted for in mass.
8. The calculated mass results for the day's ELPI recordings (measurements) averaged, and these are the results in *Table 6*.
9. The mass distribution curve of one fuel is generated by creating an average of all mass distributions from peak readings (ELPI software calculates them by default).
10. CRU parameters reported in the document are averages unless stated otherwise

1.3.3. Version 3

2. One CRU shot was directly measured by ELPI.
3. The standard CRU combustion series consist of 7 runs, and thus 7–14 ELPI measurements are made per fuel. Measurements that for some evident reason are not representative have been removed, e.g. if a valve was closed too late, air was introduced to the buffer tank, which influenced the ELPI reading.
4. Measurement peaks are selected in the ELPI software by selecting the time interval with an accuracy of 1 s.
5. The software converts current/s to mg/m^3 in the selected time interval, for all 14 impactor stages in ELPI.
6. Only stages 1–10 are accounted for in mass.
7. The calculated mass results for the day's ELPI recordings (measurements) averaged, and these are the results in *Table 8*.
8. The mass distribution curve of one fuel is generated by creating an average of all mass distributions from peak readings (ELPI software calculates them by default).
9. CRU parameters reported in the document are averages unless stated otherwise.

1.4. Results

1.4.1. Effect of averaging on mass distribution, version 2

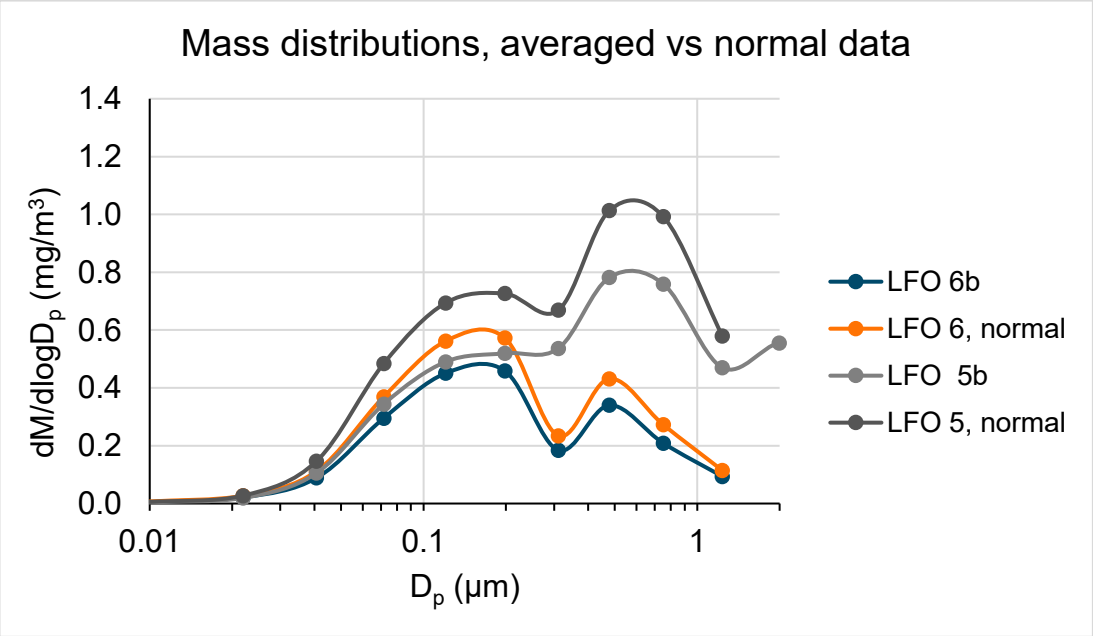

Figure 23. LFO mass distributions with and without averaging ("normal" without averaging). The total particle mass decreased with averaging.

1.4.2. Number distributions

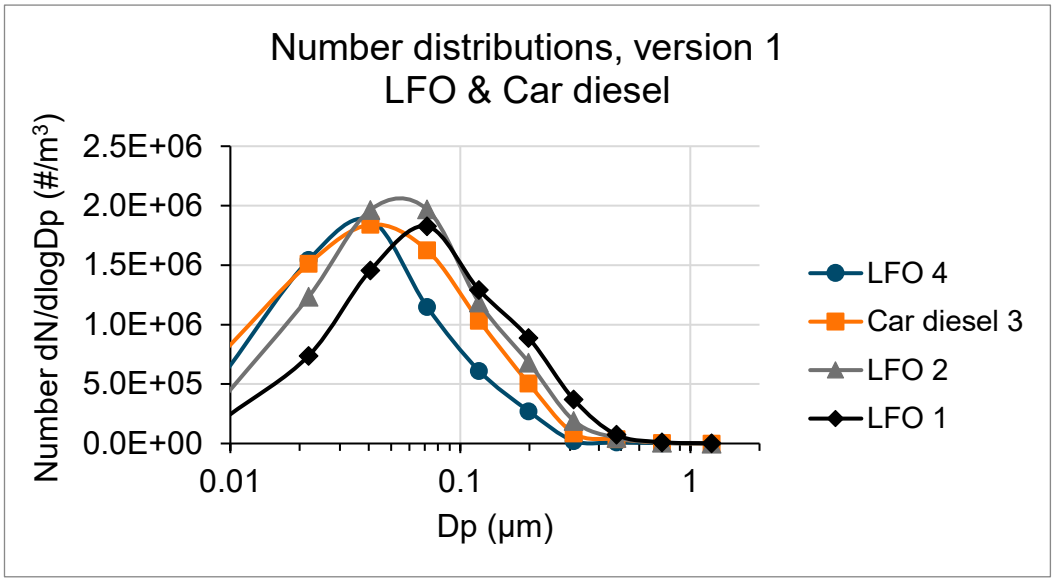

Figure 24. Particle number distribution of LFO and car diesel in version 1.

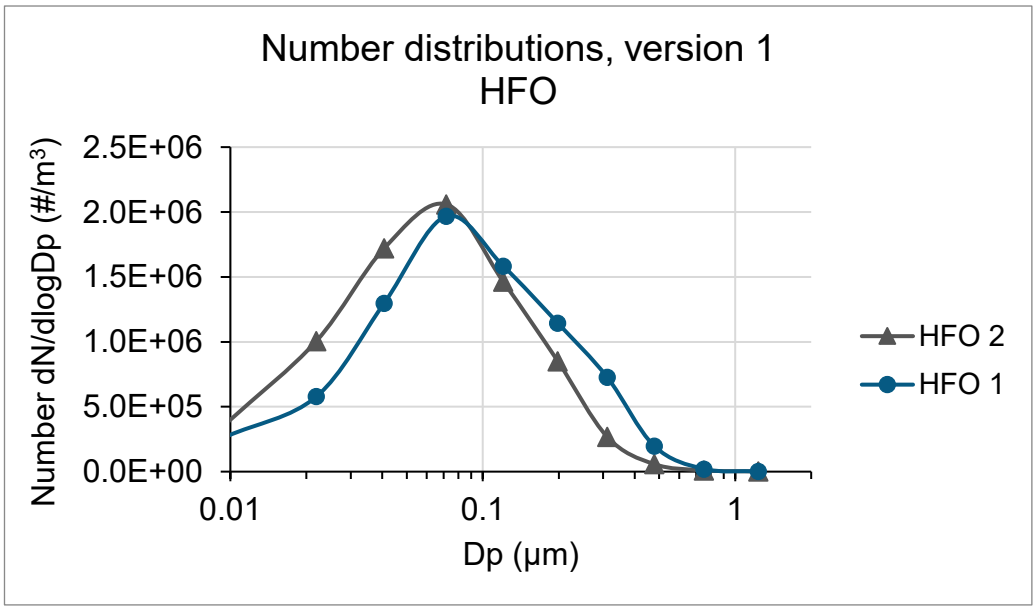

Figure 25. Particle number distribution of HFO in version 1.

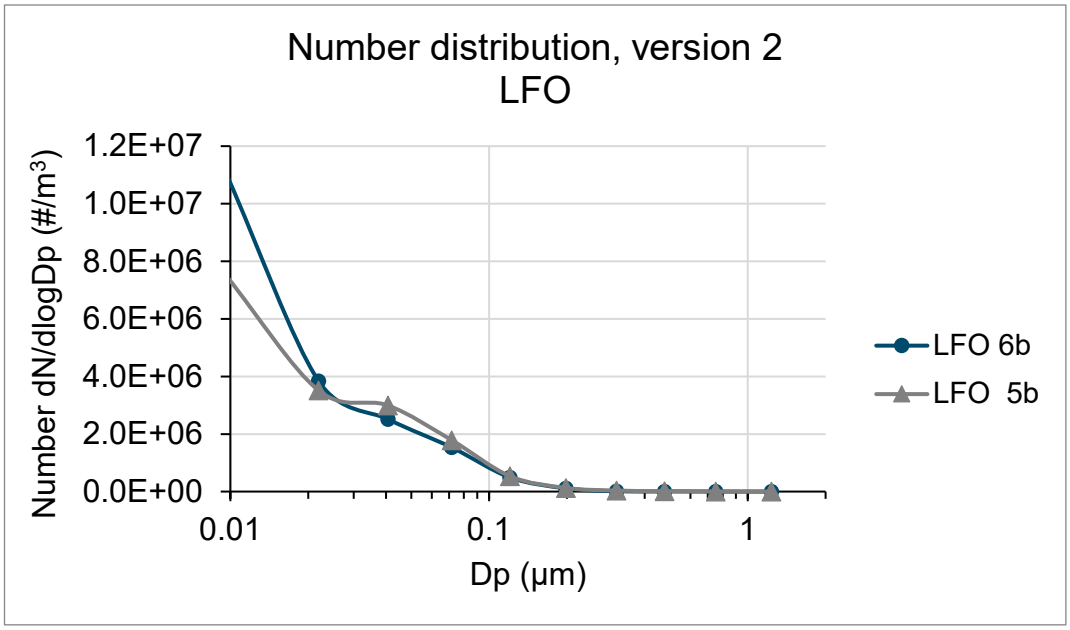

Figure 26. Particle number distribution of averaged LFO in version 2.

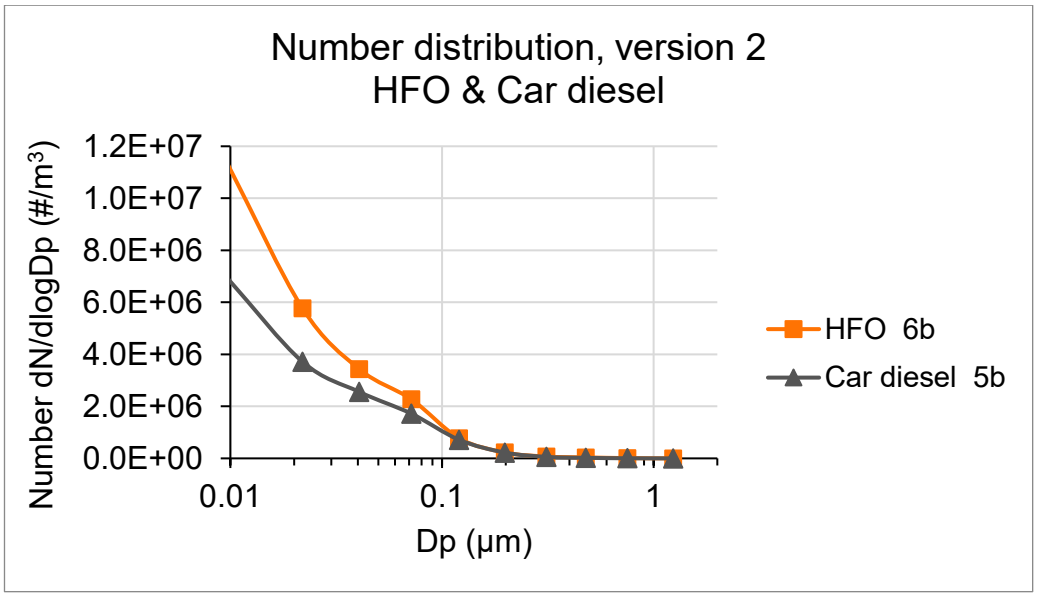

Figure 27. Particle number distribution of averaged HFO and car diesel in version 2.

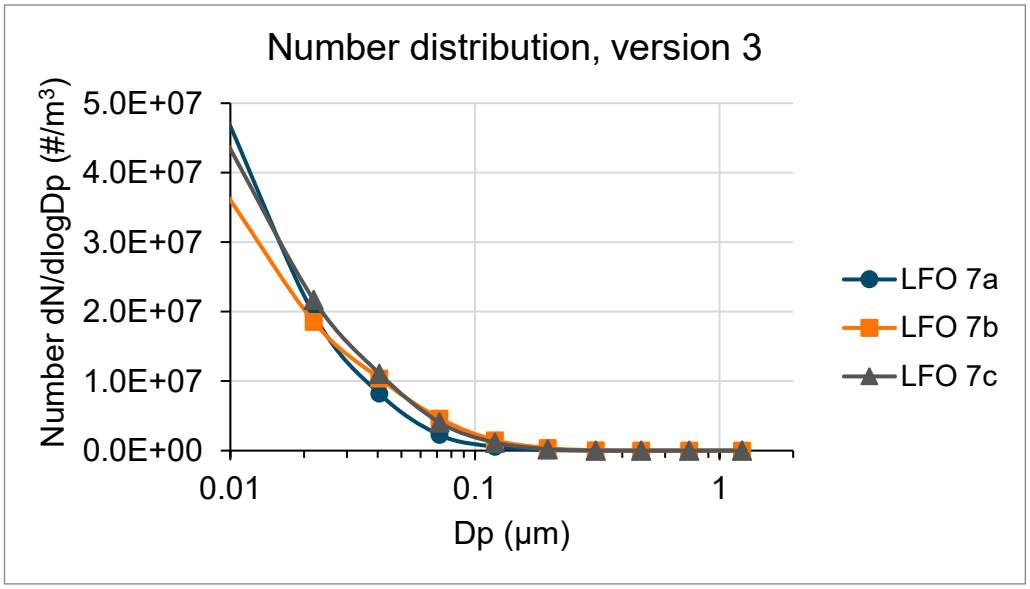

Figure 28. Particle number distribution of LFO in version 3.

1.5. Fuel analysis

1.5.1. Heavy Fuel Oil (HFO)

VPS

TEST REPORT

From : Veritas Petroleum Services (Asia) Pte Ltd
Our ref. : HR141202
Name : WARTSILA ENGINES R&D

Sample Information

Sample number : SNG1627440
Product type : Heavy Fuel oil
Description : HFO 16.08.2016 (0497902)
Sampling date : 16-Aug-2016
Sample container : VPS
Seal data : 0497902, Intact

Test Results

Test	Unit	Method	SNG1627440
Density @ 15°C	kg/m³	ISO 12185	989.6
Viscosity @ 50°C	mm²/s	ISO 3104	205.2
Viscosity @ 80°C	mm²/s	ISO 3104	44.06
Water	% V/V	ASTM D6304-C	0.01
Micro Carbon Residue	% m/m	ISO 10370	11.91
Sulfur	% m/m	ISO 8754	0.71
Total Sediment Existent	% m/m	ISO 10307-1	0.02
Total Sediment Potential	% m/m	ISO 10307-2	0.02
Ash	% m/m	LP 1001	0.038
Vanadium	mg/kg	IP 501	11
Sodium	mg/kg	IP 501	21
Aluminium	mg/kg	IP 501	4
Silicon	mg/kg	IP 501	6
Iron	mg/kg	IP 501	28
Nickel	mg/kg	IP 501	10
Calcium	mg/kg	IP 501	9
Magnesium	mg/kg	LP 1101	15
Lead	mg/kg	LP 1101	<1
Zinc	mg/kg	IP 501	<1
Phosphorus	mg/kg	IP 501	<1
Potassium	mg/kg	LP 1101	1
Pour Point, Exact	°C	ISO 3016	-9
Flash Point	°C	ISO 2719-B	101.0
Asphaltene	% m/m	ASTM D3279	5.3
Carbon	% m/m	ASTM D5291	88.00
Hydrogen	% m/m	ASTM D5291	10.35
Nitrogen	% m/m	ASTM D5291	0.42
Oxygen	% m/m	ASTM D5291 Ext	0.48

Calculated Results

Aluminium + Silicon	mg/kg	-	10
Net Specific Energy	MJ/kg	ISO 8217	40.97
Calculated Carbon Aromaticity Index	-	ISO 8217	857

Page 2 of 3

1.5.2. Light Fuel Oil (LFO)

VPS

TEST REPORT

From : Veritas Petroleum Services (Asia) Pte Ltd
Our ref. : HR141202
Name : WARTSILA ENGINES R&D

Sample Information

Sample number : SNG1619077
Product type : Distillate
Description : LFO, 07.06.2016 (0111719)
Sampling date : 07-Jun-2016
Sample container : VPS
Seal data : 0111719, Intact

Test Results

Test	Unit	Method	SNG1619077
Density @ 15°C	kg/m³	ISO 12185	840.7
Viscosity @ 40°C	mm²/s	ASTM D7042	3.663
Viscosity @ 80°C	mm²/s	ASTM D7042	1.808
Water	% V/V	ASTM D6304-C	<0.01
Micro Carbon Residue 10%	% m/m	ISO 10370	<0.10
Sulfur (Low Level)	mg/kg	ASTM D4294	<10
Total Sediment Existent	% m/m	ISO 10307-1	<0.01
Ash	% m/m	LP 1001	<0.010
Vanadium	mg/kg	IP 501	<1
Sodium	mg/kg	IP 501	<1
Aluminium	mg/kg	IP 501	<1
Silicon	mg/kg	IP 501	<1
Iron	mg/kg	IP 501	<1
Nickel	mg/kg	IP 501	<1
Calcium	mg/kg	IP 501	<1
Magnesium	mg/kg	LP 1101	<1
Lead	mg/kg	LP 1101	<1
Zinc	mg/kg	IP 501	<1
Phosphorus	mg/kg	IP 501	<1
Potassium	mg/kg	LP 1101	<1
Visual Appearance	-	LP 1902	Bright & Clear
Temp.@ 10% recovery	°C	ISO 3405	230
Temp.@ 50% recovery	°C	ISO 3405	292
Temp.@ 90% recovery	°C	ISO 3405	344
FTIR Scan 1710/1745	CM-1	LP 2401	See comment
Cloud Point	°C	ISO 3015	-1
Cold Filter Plugging Point	°C	IP 309	-12
Carbon	% m/m	ASTM D5291	86.87
Hydrogen	% m/m	ASTM D5291	13.70
Nitrogen	% m/m	ASTM D5291	<0.10
Oxygen	% m/m	ASTM D5291 Ext	<0.2
Lubricity (HFRR)	WS1,4 µm	ISO 12156-1	283
Pour Point	°C	ISO 3016	-39
Flash Point	°C	ISO 2719-A	67.0

Calculated Results

Net Specific Energy	MJ/kg	ISO 8217	42.84
Calculated Cetane Index	-	ISO 4264	56

Comments:
FTIR scan did not show any significant amounts of oxygenated compounds such as acic or esters (FAME)

Page 2 of 3

2. Engine exhaust measurement

2.1. ELPI emission calculation

	Symbol	Unit				
ISO standard conditions						
Temperature	T_norm	*K*	273			
Pressure	p_actual	*kPa*	101,3			
Ref O2 conc.	O_2,ref	*vol-%*	15			
O2 conc. in air	O_2,air	*vol-%*	21			
Measurement data, ELPI			**1**	**2**	**3**	
Duration	t_s	*min*	28	28	28	
Dust conc.	c_meas	*mg/m3*	2,10	2,78	3,07	
	Symbol	**Unit**				**Eq**
Sample #			**1**	**2**	**3**	
Exhaust gas parameters						
Oxygen content	O_2,meas	*vol-%, dry*	12,6	12,6	12,6	
Humidity	H_meas	*vol-%*	5,57	5,57	5,57	
Temperature	T_stack	*ºC*	311	315	322	
Ambient pressure	p_meas	*kPa*	101	101	101	
Volume flow in duct						
actual	Vdot_actual	*m3/h*	28386	29355	29021	
norm wet	Vdot_norm.wet	*Nm3/h*	13230	13589	13276	**1**
in norm dry	Vdot_norm.dry	*Nm3/h*	12493	12832	12537	**2**
Extracted volume						
Volume flow, ELPI	Vdot_ELPI	*L/min*	10,5	10,5	10,5	**3**
Volume flow, ELPI	Vdot_ELPI	*m3/h*	0,63	0,63	0,63	**4**
Extr. volume, ELPI	V_ELPI	*m3*	0,294	0,294	0,294	**5**
norm wet	V_ELPI.norm.wet	*Nm3*	0,137	0,136	0,134	**1**
in norm dry	V_ELPI.norm.dry	*Nm3*	0,129	0,129	0,127	**2**
Dust Concentration						
actual conditions	c_meas	*mg/m3*	2,10	2,78	3,07	**6**
norm wet	c_norm.wet	*mg/Nm3*	4,50	6,00	6,71	**7**
in norm dry	c_norm.dry	*mg/Nm3*	4,77	6,36	7,11	**8**
in 15 vol-% O2	**c_15 vol%O2**	***mg/Nm3***	**3,40**	**4,53**	**5,06**	**9**

1. Measured exhaust flow stack conditions converted to normalized temperature and pressure. For conversion of extracted volume, the volume flow is replaced by volume alone.

$$\dot{V}_{norm.wet}\left(\frac{Nm^3}{h}\right) = \dot{V}_{actual}\left(\frac{m^3}{h}\right) \cdot \frac{T_{norm}(K)}{T_{norm}\,(K) + T_{stack}(^{o}C)} \cdot \frac{p_{meas}(kPa)}{p_{actual}(kPa)}$$

2. Normalized stack air (wet) to dry. H stands for humidity.

$$\dot{V}_{norm.dry}\left(\frac{Nm^3}{h}\right) = \dot{V}_{norm.wet}\left(\frac{Nm^3}{h}\right) * (\frac{100\% - H_{meas}(vol\%)}{100\%})$$

3. Assumption: air flow through ELPI equals the air flow at probe inlet.

4. Conversion L/min to m^3/h

$$\dot{V}_{ELPI}\left(\frac{m^3}{h}\right) = \dot{V}_{ELPI}\left(\frac{L}{min}\right) \cdot 0.001\ \left(\frac{m^3}{L}\right) \cdot 60\left(\frac{min}{h}\right)$$

5. Extracted volume (m^3) during the measuring time (28 min)

$$V_{ELPI}(m^3) = \dot{V}_{ELPI}\left(\frac{L}{min}\right) \cdot t_s(min) \cdot 0.001\ \left(\frac{m^3}{L}\right)$$

6. PM measured by ELPI (mg/m^3). DR=64 already considered in the extracted value.

7. Conversion of measured PM concentration to normalized conditions (wet)

$$c_{norm.wet}\left(\frac{mg}{Nm^3}\right) = \frac{c_{meas}\left(\frac{mg}{m^3}\right) \cdot V_{ELPI}(m^3)}{V_{ELPI.norm.wet}\ (Nm^3)}$$

8. Conversion of measured PM concentration (normalized) to normalized dry conditions

$$c_{norm.dry}\left(\frac{mg}{Nm^3}\right) = \frac{c_{meas}\left(\frac{mg}{m^3}\right) \cdot V_{ELPI}(m^3)}{V_{ELPI.norm.dry}\ (Nm^3)}$$

9. Conversion of measured PM (normalized, dry) to 15 vol-% O_2

$$c_{15vol\%O2} = c_{norm.dry}\left(\frac{mg}{Nm^3}\right) \cdot \frac{O_{2,\,air}(vol\%) - O_{2,\,ref}(vol\%)}{O_{2,\,air}(vol\%) - O_{2,\,meas}(vol\%)}$$

2.2. Engine particle number distribution

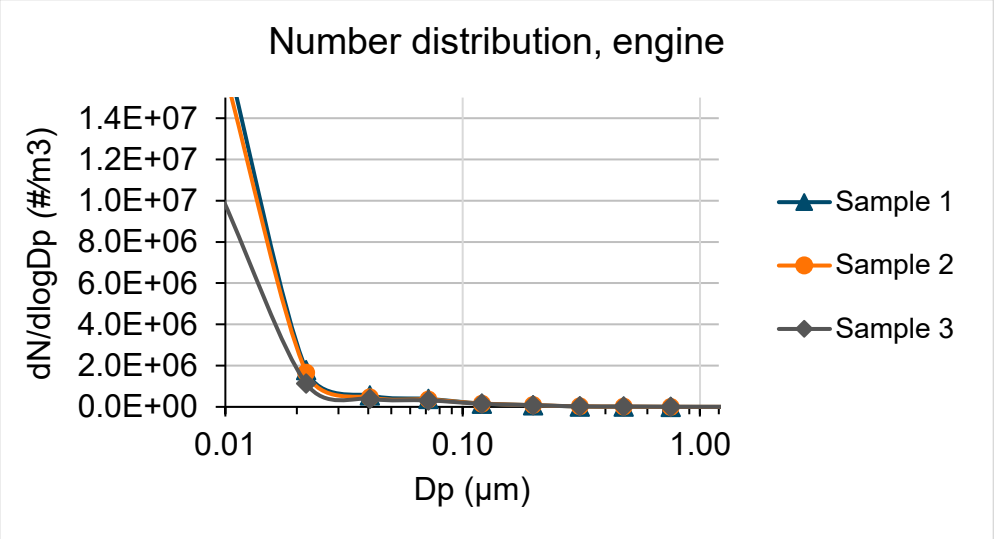

Figure 29. Particle number distribution of engine exhaust.

3. Comparison of CRU and engine emissions- calculations

3.1. Engine W6L32 PM conversion to mg/MJ

Engine data						
Energy content of fuel	LHV	*MJ/kg*	42,92			
Specific fuel consumption	SFC	*g/kWh_e*	197,12			
Engine load	L_e	*kW_e*	2808			

Fuel flow & heat rate						**Eq**
Heat rate	HR	*MJ/kWh*	8,5			**1**
Heat rate		*kJ/kWh*	8460			
Fuel flow	Fdot	*MJ/h*	23757			**2**
Fuel flow		*MJ/s*	6,6			

ISO 9096						**Eq**
Sample #			**1**	**2**	**3**	
Volume flow, duct norm dry	Vdot_norm.dry	*Nm3/h*	12506	12845	12550	**3**
[PM] norm, dry	c_norm.dry	*mg/Nm3*	12,22	11,97	11,26	**3**
Mass flow PM, duct	mdot_duct	*mg/h*	152801	153761	141363	**4**
PM per energy fuel input	mdot_fuel	*mg/MJ*	6,432	6,472	5,950	**5**
Average		***mg/MJ***		**6,28**		

ELPI						**Eq**
Sample #			**1**	**2**	**3**	
Volume flow, duct norm dry	Vdot_norm.dry	*Nm3/h*	12493	12832	12537	**3**
[PM]_norm,dry	c_norm.dry	*mg/Nm3*	4,77	6,36	7,11	**3**
Mass flow PM, duct	mdot_duct	*mg/h*	59597	81585	89104	**4**
PM per energy fuel input	mdot_fuel	*mg/MJ*	2,509	3,434	3,751	**5**
Average		***mg/MJ***		**3,23**		

1. Calculation of heat rate.

$$HR\left(\frac{MJ}{kWh}\right) = LHV\left(\frac{MJ}{kg}\right) \cdot SFC\ \left(\frac{g}{kWh\_e}\right)$$

2. Calculation of fuel flow.

$$\dot{F}\left(\frac{MJ}{h}\right) = L_e(kW_e) \cdot HR\left(\frac{MJ}{kWh}\right)$$

3. Volume flow in duct and particle mass concentration (normalized, dry) used from the previous calculation, *ELPI emission calculation*.

4. Mass flow of particles in the duct.

$$\dot{m}_{duct}\left(\frac{mg}{h}\right) = \dot{V}_{norm.dry}\left(\frac{Nm^3}{h}\right) \cdot c_{norm.dry}\left(\frac{mg}{Nm^3}\right)$$

5. Mass of particles emitted per energy fuel input.

$$PM_{fuel}\left(\frac{mg}{MJ}\right) = \dot{m}_{duct}\left(\frac{mg}{h}\right) \cdot \dot{F}\left(\frac{MJ}{h}\right)$$

3.2. CRU PM (version 1) conversion to mg/MJ

CRU & ELPI data	**Notation**	**Unit**	**Value**	**Equation**
# CRU injections per measurement			4	
Energy injected	E_test	*J*	2207	**1**
Energy injected	E_CRU	*J*	8828	**2**
Energy injected	E_CRU	*MJ*	0,0088	
Vol. flow, ELPI	Vdot_ELPI	*m3/min*	0,010	
Vol. flow, ELPI	Vdot_ELPI	*m3/s*	1,7E-04	

Equation				**3**	**4**	
Set	**Meas. #**	**Meas. duration**	**PM 1-10**	**PM 1–10**	**PM per energy fuel input**	**Average**
Notation		t_meas	c_PM	m_PM	PM_fuel	
Unit		*s*	*mg/m3*	*mg*	*mg/MJ*	*mg/MJ*
1	1	190	4,566	0,145	16,378	
1	2	190	4,167	0,132	14,946	
1	3	205	3,872	0,132	14,984	
1	4	211	3,536	0,124	14,086	
1	5	203	4,124	0,140	15,805	
1	6	205	4,115	0,141	15,926	
1	7	229	3,170	0,121	13,705	
1	8	194	3,318	0,107	12,151	**14,75**
2	1	192	4,126	0,132	14,955	
2	2	246	2,863	0,117	13,296	
2	3	205	3,100	0,106	11,996	
2	4	194	2,712	0,088	9,934	
2	5	189	2,677	0,084	9,551	
2	6	204	2,098	0,071	8,079	
2	7	197	2,334	0,077	8,679	**10,93**
3	1	189	0,891	0,028	3,180	
3	2	199	0,754	0,025	2,834	
3	3	194	0,803	0,026	2,939	
3	4	203	0,993	0,034	3,807	
3	5	206	0,878	0,030	3,415	
3	6	200	0,962	0,032	3,633	
3	7	203	1,021	0,035	3,915	
3	8	187	0,638	0,020	2,253	
3	9	199	0,742	0,025	2,787	
3	10	200	0,856	0,029	3,234	
3	11	198	1,009	0,033	3,771	
3	12	200	0,883	0,029	3,335	
3	13	196	0,962	0,031	3,560	
3	14	202	0,948	0,032	3,614	**3,31**

1. Determined previously in a test outside of this work. Mass of fuel from 10 injections was measured at an injection pressure of 1000 bar and injection period of 1000 µs. With the energy content (as LHV) of the fuel being known, energy per injection was deduced.

2. The total amount of energy injected in one measurement. Assumption: the amount of injected fuel stays constant.

3. Mass of particulates per measurement.

$$m_{PM}(mg) = c_{PM}\left(\frac{mg}{m^3}\right) \cdot t_{meas}(s) \cdot \dot{V}_{ELPI}\left(\frac{m^3}{s}\right)$$

4. Mass of particulates per energy fuel input.

$$PM_{fuel}\left(\frac{mg}{MJ}\right) = \frac{m_{PM}(mg)}{E_{CRU}(MJ)}$$

4. Mass and number distributions of ELPI measurements

4.1. CRU versions 1–3

Table 15. Raw data for version 1, mass and number distribution

Channel		1	2	3	4	5	6	7	8	9	10
Di		0,010	0,022	0,041	0,072	0,121	0,198	0,311	0,477	0,752	1,236
		Mass dM/dlogDp									
LFO	4	3,60E-04	1,02E-02	7,70E-02	2,53E-01	6,42E-01	1,25E+00	3,05E-01	6,39E-01	6,41E-01	3,56E-01
Car diesel	3	4,10E-04	9,12E-03	7,37E-02	3,67E-01	1,08E+00	2,37E+00	1,69E+00	2,39E+00	1,52E+00	7,37E-01
HFO	2	1,80E-04	5,55E-03	6,06E-02	3,96E-01	1,34E+00	3,47E+00	4,34E+00	3,31E+00	2,19E+00	1,27E+00
LFO	2	2,26E-04	7,59E-03	7,81E-02	4,33E-01	1,22E+00	3,09E+00	3,37E+00	2,99E+00	1,91E+00	9,88E-01
LFO	1	1,11E-04	4,07E-03	5,13E-02	3,51E-01	1,18E+00	3,62E+00	5,85E+00	4,22E+00	2,57E+00	1,54E+00
HFO	1	1,32E-04	3,19E-03	4,57E-02	3,79E-01	1,45E+00	4,66E+00	1,15E+01	1,13E+01	4,63E+00	2,49E+00
		Number dN/dlogDp									
LFO	4	6,27E+05	1,54E+06	1,88E+06	1,15E+06	6,12E+05	2,73E+05	2,20E+04	1,16E+04	2,86E+03	3,72E+02
Car diesel	3	8,06E+05	1,51E+06	1,84E+06	1,63E+06	1,03E+06	5,06E+05	8,64E+04	3,74E+04	6,50E+03	7,86E+02
HFO	2	3,79E+05	1,01E+06	1,72E+06	2,06E+06	1,46E+06	8,52E+05	2,68E+05	5,82E+04	9,85E+03	1,29E+03
LFO	2	4,26E+05	1,23E+06	1,97E+06	1,97E+06	1,19E+06	6,82E+05	1,92E+05	4,79E+04	8,23E+03	1,04E+03
LFO	1	2,29E+05	7,39E+05	1,46E+06	1,83E+06	1,29E+06	8,90E+05	3,71E+05	7,41E+04	1,15E+04	1,56E+03
HFO	1	2,74E+05	5,78E+05	1,30E+06	1,97E+06	1,58E+06	1,14E+06	7,27E+05	1,98E+05	2,08E+04	2,52E+03

Table 16. Mass and number distribution of version 2. "Avg" signifies averaged values over a period of 10 seconds of the "normal" values

Channel			1	2	3	4	5	6	7	8	9	10
Di			0,010	0,022	0,041	0,072	0,121	0,198	0,311	0,477	0,752	1,236
			Mass dM/dlogDp									
LFO	6b	avg	5,29E-03	2,12E-02	8,86E-02	2,95E-01	4,51E-01	4,59E-01	1,84E-01	3,40E-01	2,09E-01	9,37E-02
LFO	6	normal	6,62E-03	2,69E-02	1,12E-01	3,70E-01	5,62E-01	5,73E-01	2,34E-01	4,32E-01	2,72E-01	1,14E-01
HFO	6b	avg	5,46E-03	3,18E-02	1,21E-01	4,37E-01	7,08E-01	9,26E-01	1,13E+00	2,14E+00	2,28E+00	6,39E-01
HFO	6	normal	7,11E-03	4,19E-02	1,60E-01	5,79E-01	9,36E-01	1,22E+00	1,48E+00	2,80E+00	2,94E+00	7,00E-01
Car diesel	5b	avg	3,34E-03	2,05E-02	9,00E-02	3,31E-01	6,54E-01	9,11E-01	9,23E-01	1,20E+00	9,90E-01	3,66E-01
Car diesel	5	normal	4,39E-03	2,72E-02	1,19E-01	4,39E-01	8,71E-01	1,21E+00	1,22E+00	1,58E+00	1,27E+00	4,07E-01
LFO	5b	avg	3,60E-03	1,94E-02	1,05E-01	3,44E-01	4,90E-01	5,20E-01	5,37E-01	7,82E-01	7,59E-01	4,70E-01
LFO	5	normal	5,08E-03	2,74E-02	1,47E-01	4,84E-01	6,94E-01	7,26E-01	6,69E-01	1,01E+00	9,92E-01	5,79E-01
			Number dN/dlogDp									
LFO	6b	avg	1,10E+07	3,84E+06	2,52E+06	1,54E+06	4,92E+05	1,13E+05	1,16E+04	5,96E+03	9,36E+02	9,48E+01
LFO	6	normal	1,37E+07	4,87E+06	3,17E+06	1,92E+06	6,13E+05	1,41E+05	1,48E+04	7,57E+03	1,22E+03	1,16E+02
HFO	6b	avg	1,13E+07	5,77E+06	3,43E+06	2,27E+06	7,72E+05	2,27E+05	7,16E+04	3,76E+04	1,02E+04	6,46E+02
HFO	6	normal	1,47E+07	7,60E+06	4,53E+06	3,01E+06	1,02E+06	2,99E+05	9,37E+04	4,92E+04	1,32E+04	7,08E+02
Car diesel	5b	avg	6,91E+06	3,72E+06	2,56E+06	1,72E+06	7,14E+05	2,23E+05	5,84E+04	2,11E+04	4,44E+03	3,70E+02
Car diesel	5	normal	9,07E+06	4,93E+06	3,37E+06	2,28E+06	9,50E+05	2,98E+05	7,70E+04	2,78E+04	5,70E+03	4,11E+02
LFO	5b	avg	7,45E+06	3,51E+06	2,99E+06	1,79E+06	5,35E+05	1,28E+05	3,40E+04	1,37E+04	3,41E+03	4,75E+02
LFO	5	normal	1,05E+07	4,97E+06	4,16E+06	2,52E+06	7,57E+05	1,78E+05	4,23E+04	1,78E+04	4,45E+03	5,86E+02

Table 17. Raw data of version 3, mass and number distribution

Channel		1	2	3	4	5	6	7	8	9	10
Di		0,010	0,022	0,041	0,072	0,121	0,198	0,311	0,477	0,752	1,236
		Mass dM/dlogDp									
LFO	7a	2,30E-02	1,08E-01	2,89E-01	4,35E-01	5,17E-01	4,02E-01	1,93E-01	4,16E-02	0	0
LFO	7b	1,77E-02	1,02E-01	3,66E-01	8,92E-01	1,38E+00	1,53E+00	9,12E-01	7,63E-02	0	0
LFO	7c	2,13E-02	1,20E-01	3,91E-01	7,81E-01	1,07E+00	8,89E-01	3,75E-01	0	0	0
		Number dN/dlogDp									
LFO	7a	4,76E+07	1,96E+07	8,21E+06	2,26E+06	5,64E+05	9,87E+04	1,22E+04	7,30E+02	0	0
LFO	7b	3,67E+07	1,85E+07	1,04E+07	4,64E+06	1,51E+06	3,76E+05	5,78E+04	1,34E+03	0	0
LFO	7c	4,42E+07	2,17E+07	1,11E+07	4,06E+06	1,16E+06	2,18E+05	2,38E+04	0	0	0

4.2. W6L32 ELPI measurement

Table 18. Mass and number distribution of engine measurements with ELPI

Channel	1	2	3	4	5	6	7	8	9	10
Di	0,010	0,022	0,041	0,072	0,121	0,198	0,311	0,477	0,752	1,236
	Mass dM/dlogDp									
Sample 1	2,05E-02	3,46E-02	7,78E-02	3,10E-01	6,89E-01	1,53E+00	1,69E+00	3,30E+00	2,69E+00	1,27E-01
Sample 2	1,91E-02	3,23E-02	6,48E-02	2,83E-01	6,92E-01	1,58E+00	2,08E+00	3,76E+00	3,37E+00	1,77E+00
Sample 3	1,16E-02	2,19E-02	5,43E-02	2,53E-01	6,36E-01	1,52E+00	2,12E+00	4,16E+00	3,98E+00	2,31E+00
	Number dN/dlogDp									
Sample 1	1,8E+07	1,8E+06	5,6E+05	3,9E+05	1,6E+05	8,2E+04	1,9E+04	1,1E+04	2,4E+03	3,0E+01
Sample 2	1,7E+07	1,7E+06	4,6E+05	3,5E+05	1,6E+05	8,5E+04	2,3E+04	1,3E+04	3,0E+03	4,2E+02
Sample 3	1,0E+07	1,1E+06	3,9E+05	3,1E+05	1,5E+05	8,2E+04	2,3E+04	1,4E+04	3,5E+03	5,5E+02